

**Determination of the  
surface sensible heat flux  
from the structure parameter  
of temperature at 60 m height  
during day-time**

*Miranda Braam*

**KNMI technical report = technisch rapport; TR-303**

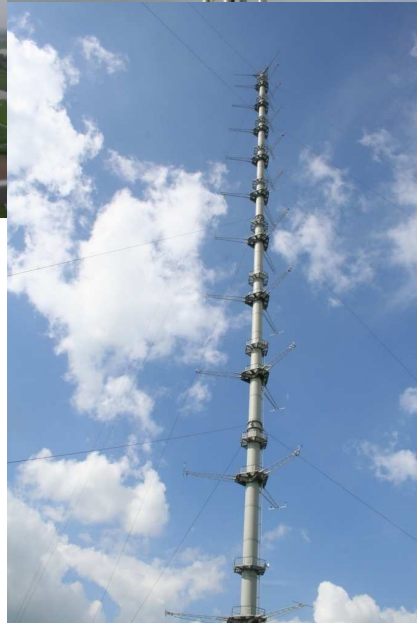
De Bilt, 2008

PO Box 201  
3730 AE De Bilt  
Wilhelminalaan 10  
De Bilt  
The Netherlands  
<http://www.knmi.nl>  
Telephone +31(0)30-220 69 11  
Telefax +31(0)30-221 04 07

Author: Braam, M..



# Determination of the Surface Sensible Heat Flux from the Structure Parameter of Temperature at 60 m height during day-time.



Miranda Braam  
MSc-student Meteorology and Air Quality  
Wageningen University  
Internship report: October 2008

Supervisor KNMI: Fred C. Bosveld  
Supervisor WUR: Arnold F. Moene



## Abstract

Recently a scintillometer is installed at 60 m height at Cabauw to determine the surface sensible heat flux. Since 60 m is not located in the surface layer the entire day, the applicability of Monin Obukhov Similarity Theory (MOST) is questionable. Therefore, in this research two different theoretical concepts to determine the surface sensible heat flux from the structure parameter of temperature ( $C_T^2$ ) obtained from a scintillometer at 60 m under unstable conditions are investigated. The first concept assumes that  $C_T^2$  at 60 m has to be scaled with the 60 m heat flux, whereas the second concept assumes that  $C_T^2$  at 60 m has to be scaled with the surface heat flux. To ensure comparable footprints of  $C_T^2$  and the turbulent heat flux;  $C_T^2$  is calculated from the sonic anemometer/ thermometer observations at 60 m height instead of using scintillometer data. Data from sonic anemometer/ thermometer systems at 3 m, 100 m and 180 m are investigated as well.

By analyzing the fluxes at the four levels, we found that the 3 m temperature flux deviates from the for flux divergence corrected fluxes at the other levels. The observed structure parameter at 3 m follows the one calculated with MOST, as expected because 3 m lies in the surface layer the entire day. The observations of 60 m show that neither of the two concepts is fully supported by the observations. The moment of the morning transition is measured at the same time for the local flux and the local structure parameter. Further, in the morning period the use of the surface sensible heat flux show the best result. On the other hand, in the afternoon when MOST has to be valid, the two methods differ a lot and the use of the local flux is the best option, which is caused by the deviation of the 3 m sensible heat flux. Therefore, we have done the same analysis with the surface flux derived from the 60 m flux corrected for temperature storage below 60 m. These results are the same as before for the moment of transition, however, in the morning period the observed  $C_T^2$  lies between the two of MOST and in the afternoon all the structure parameters are comparable. Increasing of height, result in less correlation between observed and calculated  $C_T^2$  and an increase in the underestimation of the calculated  $C_T^2$ . Perhaps, other processes than surface processes play a role as well.

Keywords: Structure parameter of temperature, Turbulent sensible heat flux, Monin Obukhov Similarity Theory, Sonic anemometer/ thermometer, Scintillometer

## Preface

Part of the MSc study Meteorology and Air Quality (Wageningen University) is an internship. I have done my internship at the KNMI at the department of Regional Climate, which is part of the sector Climate and Seismology, in the period from April till August 2008. In this report I present the results of my research for my internship. My supervisor was Fred Bosveld, and I want to thank him for all the support he has given me during these months. I have learnt a lot in this period. But next to the learning, I enjoyed also the time at the KNMI. The coffee and lunch breaks with all the colleagues were nice. I am also grateful that Fred 'persuaded' me to present the results of this research at the EMS Conference 2008 in Amsterdam. Though, it was very exciting for me and I was of course nervous, the presentation went well. Of course, it was a good way to train my presentation skills, as well. Overall, it was a nice experience that I will never forget.

I want also thank Arnold Moene from Wageningen University for the support, especially for the critical feedback on the report.

Finally, I thank Henk Klein Baltink (KNMI) to provide the data of the boundary layer height, and Eddy Moors (Alterra WUR) for the use of the 100 m turbulent data.

# Contents

Abstract .....	1
Preface .....	2
Contents .....	3
1. Introduction .....	4
2. Theory .....	6
2.1 Turbulence .....	6
2.2 Structure function and structure parameter .....	7
2.3 Monin Obukhov Similarity Theory .....	9
3. Data .....	11
3.1 The sonic anemometer/ thermometer .....	11
3.2 The scintillometer .....	13
3.3 Data for MOST .....	14
3.4 Selection of the data .....	14
4. Results and Discussion .....	15
4.1 Defining the inertial sub range .....	15
4.2 Boundary layer development: Boundary layer height and turbulent temperature fluxes .....	17
4.3 The structure parameter of temperature at 3 m .....	19
4.4 The structure parameter of temperature at 60 m .....	23
4.5 The structure parameter of temperature at the other heights .....	28
4.6 The structure parameter of temperature at 60 m revised .....	31
5. Conclusions and Recommendations .....	34
6. Literature .....	36

# 1. Introduction

Optical scintillometers can be used to determine the area averaged surface fluxes of sensible heat, which are of interest for many meteorological and hydrological studies. Area averaged surface fluxes are of interest for the evaluation of atmospheric models and satellite based retrieval algorithms. Recently an extra Large Aperture Scintillometer (XLAS) of Kipp & Zonen has been set up over a 10 km path between the Cabauw Tower (51°58'.22 N, 4°55'.57 E) and the TV tower of IJsselstein (52°00'.72 N, 5°03'.23 E) in the Netherlands at about 60 m above the surface. This large height is chosen to avoid saturation of the scintillometer signal (Kohsiek et al. 2002; Kohsiek et al. 2006). From the scintillometer data the structure parameter of refractive index of air is determined, which is used to calculate the structure parameter of temperature. Normally the surface sensible heat flux is derived by applying Monin Obukhov Similarity Theory (MOST) (Wyngaard et al. 1971, Wyngaard 1973, Moene et al. 2004, Meijninger 2003, and others). This similarity theory is defined for the surface layer, where fluxes are assumed to be constant with height. Due to the large height of the XLAS path at Cabauw, the observations are not always located in the surface layer. This is especially the case in the morning when boundary layer height is relatively small. In that case the application of MOST can be questioned. Two different theoretical concepts to obtain the surface sensible heat flux from the structure parameter of temperature at 60 m are investigated:

- The structure parameter at 60 m has to be scaled with the turbulent sensible heat flux at 60 m instead of the surface flux. The assumption is that there is a local relation between vertical heat transport and the smaller scale fluctuations in the turbulent cascade towards the dissipation range. To obtain the true surface heat flux a correction for the energy that is used to heat the column below the 60 m has to be applied.
- The structure parameter at 60 m has to be scaled with the surface heat flux. Here it is assumed that the surface heat flux is the driving force for the largest thermals, which are as large as the depth of the boundary layer. These large thermals are broken into smaller eddies, which determines the structure parameter throughout the boundary layer. Consequently, we assume that Monin Obukhov similarity theory can be stretched to higher levels in this case.

We test the concepts with sonic anemometer/thermometer observations from the Cabauw tower for a number of clear convective days in May 2008. The structure parameter for temperature at 60 m is derived from the sonic anemometer/thermometer after careful correction for small-scale attenuation. Subsequently the structure parameter is compared with the surface sensible heat flux and the flux at 60 m. The sonic anemometer/thermometer at the tower is used and not the scintillometer, to minimize problems of a different footprint between the turbulent sensible heat flux observations and at the structure parameter of temperature, since the XLAS measured along a path, whereas the tower measurements are local. To complete this study, heat fluxes and structure parameters derived from the sonic anemometer/ thermometers located at other levels at the Cabauw Tower (3 m, 100 m and 180 m) are investigated as well.

The main research question is as follows:

- How should the surface fluxes be calculated from the structure parameter of temperature determined at 60 m under unstable conditions, especially for the morning period if the 60 m level is situated above the surface layer?

With the next sub questions:

- Does the structure parameter that is determined at 60 m, 100 m or 180 m correlate better with the turbulent sensible heat fluxes at the respective location or with the surface fluxes? Or in other

words, is the structure parameter at the respective level more sensitive to local turbulent transport around that level, or more sensitive to turbulent processes at the surface?

- Are the observed values for the structure parameter at 60 m, 100 m or 180 m more comparable with the structure parameter calculated with MOST from the turbulent sensible heat flux at the respective level or the one calculated with MOST from the turbulent heat flux at the surface?
- Do the sonic anemometer at 60 m and the scintillometer, which is also situated at 60 m, give comparable values for the structure parameter of temperature?

In chapter 2 some theory about turbulence, structure parameter and MOST is given. Information about the set-up, the dataset and the applied corrections can be found in chapter 3. In chapter 4, the results are presented and discussed. Finally, the conclusions and some recommendations are given in the last chapter.

## 2. Theory

### 2.1 Turbulence

In the convective atmospheric boundary layer, the main process to transport heat, moisture and momentum is turbulent transport. Some features of atmospheric turbulent transport are (de Bruin, 2005; Moene and van Dam, 2008; Stull, 1988):

- Turbulent transport is irregular and chaotic in space and time.
- Turbulent transport consist of rotational three-dimensional whorls of various sizes, called eddies. The largest eddies have the same order of magnitude as the boundary layer depth.
- Turbulent transport is diffusive, which causes that heat, moisture and momentum is efficiently well mixed in the whole boundary layer.
- Turbulent transport has large Reynolds numbers.
- Turbulent transport is dissipative: large eddies generated by wind shear and buoyancy are broken into smaller eddies (energy cascade process), which results in energy at the larger scales being dissipated into heat at smallest scales (Kolmogorov micro scale:  $\eta = (\nu^3/\varepsilon)^{1/4}$ , in which  $\nu$  is the kinematic molecular viscosity and  $\varepsilon$  is the dissipation rate).

A consequence of the dissipative feature of turbulent transport is that one distinguished turbulence in different length scales. Eddies with a length scale ( $l$ ), much smaller than the large scales and larger than the smallest scales, are situated in the inertial sub range ( $l_0 \ll l \ll L_0$ , in which  $l_0$ , the inner scale, is related to the Kolmogorov micro scale:  $l_0 = 7.4\eta$  and  $L_0$  is the outer scale). In this range, energy is only inertial transferred from large to small scales, and neither produced nor dissipated. Consequently, neither the inner scale nor the outer scale plays a role in the dimensionless analysis in this range. By applying dimensionless analysis, it can be found that in the inertial sub range the relation between the one dimensional temperature spectrum ( $\phi_T$ ) and the wave number ( $\kappa$ ) has the form of:  $\phi_T \propto \kappa^{-5/3}$ , which is sometimes called the -5/3 behaviour (Nieuwstadt, 1998).

Because of the irregular and chaotic feature of turbulence, statistical techniques are needed to describe turbulence. Often the variance and covariance are used to describe turbulence; however, for this study we are interested in the structure function and structure parameter. Another consequence of the above described features of turbulence is that the processes are non-local. This means that turbulence depends not only on the local atmospheric variables, but also on atmospheric conditions at other locations and at other times, due to the mixing of air by eddies with scales that range over several orders of magnitudes. In the surface layer, the dominant processes of turbulent production at a certain level are the processes at the surface, whereas processes in the rest of the boundary layer, such as entrainment processes, play a less dominant role. The surface layer is defined as the lowest 10% of the boundary layer. In this layer the turbulent fluxes are assumed almost constant with height; the fluxes differ not more than 10% of the surface fluxes. Therefore, another name for this layer is the constant flux layer. The lowest part of the surface layer is the roughness sub layer; here the influences of roughness obstacles on the mean profiles are visible. In the layer above, sometimes called the inertial sub layer, these influences on the mean quantities are not visible anymore. The log-linear shape of the wind profile under neutral conditions characterizes this layer. Furthermore, MOST can be used in this layer (de Bruin, 2005; Moene and van Dam, 2008; Stull, 1988).

## 2.2 Structure function and structure parameter

As mentioned before, we use the structure function to describe the statistical properties of turbulence. The structure function for temperature is defined as the average (in time or space) of the square of the temperature difference between two measurements. The structure function of temperature ( $D_{TT}$ ) between two measurements in space is defined as (Stull, 1988; Bosveld, 1999; Moene et al., 2004; Meijninger, 2003; Wyngaard, 1973):

$$D_{TT_s}(r) = \overline{(T(x+r) - T(x))^2} \quad (1)$$

in which the subscript s indicates that it is the spatial structure function,  $T(x)$  and  $T(x+r)$  is the temperature of the two measurements in space, and  $r$  is the spatial separation between the measurements. For spatial separation that are situated in the inertial sub range ( $l_0 < r < L_0$ ), similarity theory gives a relation between the structure function and structure parameter ( $C_T^2$ ):

$$D_{TT_s}(r) = C_T^2 \cdot r^{2/3} \quad (2)$$

The relation of equation 2 indicates that in the inertial sub range the structure function is proportional to the spatial separation, in which the structure parameter is the proportion constant. The structure parameter of temperature corresponds to temperature fluctuations, for this reason, minimum values of  $C_T^2$  should be found if the turbulent sensible heat flux is zero. This occurs around sunrise and sunset, when the boundary layer is neutral. Because, most of the temperature fluctuations are in the lower part of the boundary layer, the  $C_T^2$  decreases with height.

The structure function of temperature in time is defined as follows:

$$D_{TT_t}(\tau) = \overline{(T(t+\tau) - T(t))^2} \quad (3)$$

in which the subscript t indicates that it concerns the temporal structure function,  $T(t)$  and  $T(t+\tau)$  is the temperature of the two measurements in time, and  $\tau$  is the time lag between the two measurements.

The temporal structure function can be calculated with a sonic anemometer/ thermometer. However, often the spatial structure function and especially the spatial structure parameter are of interest. To derive the spatial structure function from the temporal structure function, we have to convert from time coordinates to space coordinates. By (a) assuming stationary and horizontal homogeneous conditions, (b) applying Taylor hypothesis and (c) assuming that the deviation of the wind vector has a three dimensional Gaussian distribution, Bosveld (1999) converts the coordinates systems as follows:

$$D_{TT_s}(r) = \frac{D_{TT_t}(\tau)}{\left(1 - \frac{1}{9} \frac{\sigma_u^2}{\bar{U}^2} + \frac{1}{3} \frac{\sigma_v^2}{\bar{U}^2} + \frac{1}{3} \frac{\sigma_w^2}{\bar{U}^2}\right)} = \frac{D_{TT_t}(r/\bar{U})}{\left(1 - \frac{1}{9} \frac{\sigma_u^2}{\bar{U}^2} + \frac{1}{3} \frac{\sigma_v^2}{\bar{U}^2} + \frac{1}{3} \frac{\sigma_w^2}{\bar{U}^2}\right)} \quad (4)$$

in which,  $\sigma_{u,v,w}^2$  is the variance of respectively the deviation of the main wind vector in the u, v and w direction and  $\bar{U}$  is the length of the averaged wind vector ( $\sqrt{\langle U(t) \rangle^2 + \langle V(t) \rangle^2}$ ).

To calculate the structure parameter of temperature ( $C_T^2$ ) from the structure parameter of the refractive index of air ( $C_n^2$ ), which is determined from the scintillometer measurements, the next assumption can be used (Meijninger, 2003; Moene et al., 2004):

$$C_T^2 \approx C_n^2 \cdot \frac{T^2}{A_T^2} \left(1 + \frac{0.03}{\beta}\right)^{-2} \quad (5)$$

in which  $\beta$  is the Bowen ratio and  $A_T^2$  is a function of the wavelength and the mean values of temperature, humidity and atmospheric pressure. The factor  $\left(1 + \frac{0.03}{\beta}\right)^{-2}$  is called the Bowen correction, which is a correction for humidity related scintillations.

For a wavelength in the near infrared region, the function is as follow (Andreas, 1988):

$$A_T = -0.78 \cdot 10^{-6} \cdot \frac{P}{T} + 0.126 \cdot 10^{-6} R_v \cdot \rho_v \approx -0.78 \cdot 10^{-6} \cdot \frac{P}{T} \quad (6)$$

in which  $P$  is the pressure,  $R_v$  the specific gas constant for water vapour ( $461.5 \text{ J K}^{-1} \text{ kg}^{-1}$ ) and  $\rho_v$  is the absolute humidity.

### 2.3 Monin Obukhov Similarity Theory

From the spatial structure parameter of temperature the turbulent sensible heat flux can be calculated by applying the Monin Obukhov Similarity Theory (MOST). MOST is determined for the inertial sub layer under stationary and homogeneous conditions. MOST is derived from the observation that the statistical structure of turbulence in the surface layer is fully determined by three parameters,  $u_*$  the friction velocity,  $\frac{g}{T} \overline{w'T'}$  the buoyancy surface flux and  $z$  the height from the surface. In MOST, the following equations are used, in which equation 8 till 10 are the definitions in MOST and equation 7 is an example how the structure parameter of temperature can be scaled:

$$\frac{C_T^2(z)^{2/3}}{T_*^2} = f\left(\frac{z}{L_{Ob}}\right) \quad (7)$$

$$T_* = -\frac{\overline{w'T'}}{u_*} \quad (8)$$

$$u_* = \sqrt[4]{\overline{u'w'^2} + \overline{v'w'^2}} \quad (9)$$

$$L_{Ob} = \frac{Tu_*^2}{\kappa g T_*} = \frac{Tu_*^3}{\kappa g \overline{w'T'}} \quad (10)$$

in which  $T_*$  is the temperature scale,  $L_{Ob}$  is the Obukhov Length,  $\overline{w'T'}$  is the kinematic turbulent sensible heat flux, because of the kinematic form we will call this flux the turbulent temperature flux from now on,  $\overline{u'w'}$  and  $\overline{v'w'}$  are the turbulent momentum flux in respectively u- and v-direction,  $\kappa = 0.4$  is the von Karman constant and  $g = 9.81 \text{ms}^{-1}$  is the gravity acceleration. Several expressions for  $f\left(\frac{z}{L_{Ob}}\right)$  exist in literature for stable and unstable conditions (Wyngaard 1973; Hill et al. 1992; Andreas 1988; de Bruin et al. 1993, for an overview see Moene et al. 2004). For unstable conditions the equations are given in Table 1 and Figure 1.

The structure parameter of temperature obtained from the structure function as described in section 2.2 is compared with those obtained from MOST. To investigate if the structure parameter of temperature at a respective level is more sensitive to turbulent transport around that level or to turbulent processes at the surface, MOST is applied in two different ways. In the first way the structure parameter of temperature the surface turbulent fluxes are used (MOSTs). This is the standard way of using the MOST. By using MOSTs we assume that the surface is the driving force for thermals in the boundary layer. Since the large influences of the surface, we assume that MOST can be stretched to higher levels. On the other hand, the second method (MOSTI) calculates with the turbulent fluxes at 60 m, 100 m or 180 m. This way of using MOST is comparable with the local scaling hypothesis that is often used in the stable boundary layer (Nieuwstadt, 1984).

Table 1 Several expressions for the similarity function under unstable conditions

The expression for $f\left(\frac{z}{L_{Ob}}\right)$	The references
$f\left(\frac{z}{L_{Ob}}\right) = 4.9 \cdot \left(1 - 7 \frac{z}{L_{Ob}}\right)^{-2/3}$	Wyngaard (1973)
$f\left(\frac{z}{L_{Ob}}\right) = 4.9 \cdot \left(1 - 6.1 \frac{z}{L_{Ob}}\right)^{-2/3}$	Andreas (1988)
$f\left(\frac{z}{L_{Ob}}\right) = 8.1 \cdot \left(1 - 15 \frac{z}{L_{Ob}}\right)^{-2/3}$	Hill et al. (1992)
$f\left(\frac{z}{L_{Ob}}\right) = 4.9 \cdot \left(1 - 9 \frac{z}{L_{Ob}}\right)^{-2/3}$	De Bruin et al. (1993)

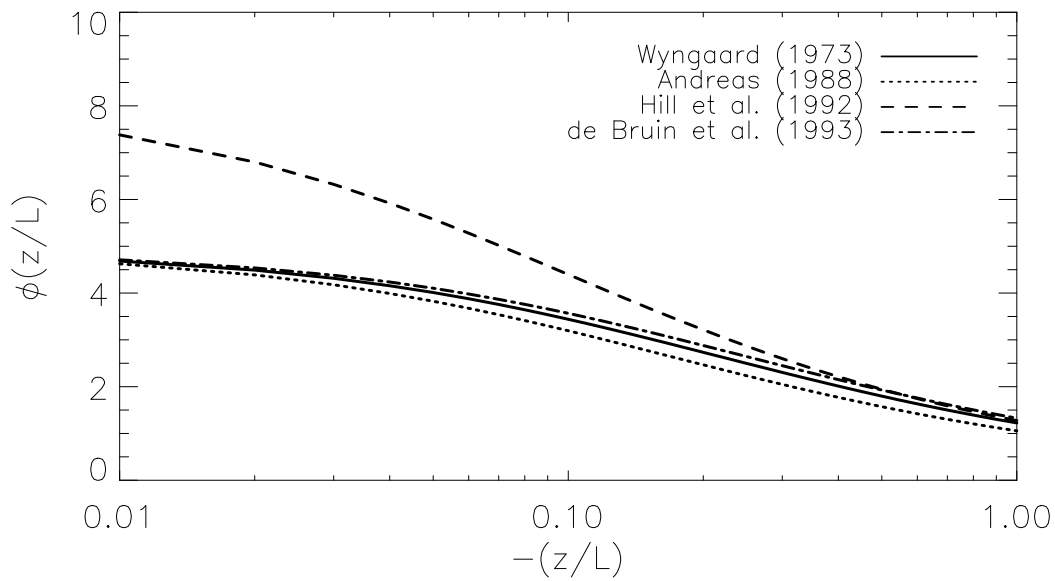


Figure 1 The equations for the similarity function under unstable conditions, as given in Table 1.

### 3. Data

The data have been measured at the Cabauw tower (51°58'.22 N, 4°55'.57 E) in the western part of the Netherlands. The area around the tower is an open pasture terrain for 400m (Van Ulden en Wieringa, 1996). The analyzed period is from 3 May 2008 till 11 May 2008. This period is chosen, because it consists of cloud free days, and the synoptic weather conditions show only a little variation.

The data is processed in Mobibase 'A database system for micro meteorological observations' (for more information about Mobibase see: <http://www.knmi.nl/~bosveld>). From Mobibase all the in-situ observations are available, averaged over 10 and 30 minutes. We used the 30 minutes averaged data, unless otherwise noted.

#### 3.1 The sonic anemometer/ thermometer

##### Set-up

The sonic anemometer/ thermometer (Gill Solent R3, sample frequency: 10Hz) is used (a) to calculate the turbulent fluxes and (b) to obtain the structure function of temperature, as described in section 2. The sonic path has a distance (L) of 0.15m. Four of these sonic anemometer/ thermometers are installed at respectively 3, 60, 100 and 180 m height. The one at 3 m is located at a small mast approximately 200m north of the main tower. The other turbulence instruments are placed at the South-East booms of the tower. With easterly winds, as in the case for the period analyzed here, no significant tower flow obstruction occurs.

##### Data processing

The temperature and the turbulent temperature flux calculated from the sonic anemometer/ thermometer observations have to be corrected for wind speed and humidity (Schotanus et al. 1983; Liu et al. 2001; Gill Instruments Ltd., 2002). The wind speed correction is already internally done in the instrument, according to equation 21 from appendix C of Gill Instruments Ltd. (2002). To correct the turbulent heat flux for humidity only, we use the first part of equation 12 of Liu (2001):

$$\overline{w'T'_c} = \overline{w'T'_s} - 0.51\overline{w'q'_s}T \quad (11)$$

in which the primes are the fluctuation.

For the turbulent temperature fluxes tilt correction are applied as well (Lee et al. 2004). The 3 m turbulent flux is also corrected for low frequency loss due to a finite averaging, whereas at the other levels this is neglected because the correction is small (Bosveld, 1999).

To determine the structure function of temperature, humidity corrections as in equation 1 of Liu have to be applied. However, the temperature from the sonic anemometer/ thermometer and the humidity measured by a Licor show always a bias compared to the true temperature and humidity. This bias does not vary over time intervals used here to determine the structure function. Consequently, this observation can directly be used to derive the structure function:



Figure 2 The sonic anemometer/ thermometer at 3 m.

$$(T_c(t+\tau) - T_c(t))^2 = (T'_c(t+\tau) - T'_c(t))^2 \quad (12)$$

According to Liu et al. (2001), the temperature fluctuation corrected for humidity is:

$$T'_c = T'_s - 0.51q'\bar{T} \quad (13)$$

in which  $T'_c$  is the corrected temperature fluctuation,  $T'_s$  is the temperature fluctuation measured from the sonic anemometer/ thermometer,  $q'$  is the specific humidity,  $\bar{T}$  is the mean temperature. The correction for the structure function of temperature now becomes:

$$\begin{aligned} [T_c(t+\tau) - T_c(t)]^2 &= [T'_s(t+\tau) - T'_s(t) + 0.51\bar{T}(q'(t) - q'(t+\tau))]^2 \\ &= [T'_s(t+\tau) - T'_s(t) + 0.51\bar{T}(q(t) - q(t+\tau))]^2 \end{aligned} \quad (14)$$

The mean air temperature is measured with KNMI Pt500-elements at 200, 140, 80, 40, 20, 10 and 1.5 m. To determine the temperature at 3 m, 60 m, 100 m and 180 m a linear interpolation between the two nearest levels is done. The specific humidity fluctuations are obtained by an open path sensor measuring humidity and CO<sub>2</sub> open path sensor, the Licor 7500. Licors are placed at the same height as the sonic anemometer/ thermometer.

Initially, the temporal structure function of temperature is determined for fixed time lags varying from 0.1 s to 2 s. Consequently, the spatial separation ( $r = \tau \cdot \bar{U}$ ) varies in time after conversion of the temporal structure function of temperature to the spatial structure function according to equation 4. The length of the averaged wind vector and the variance of the main wind vector are also determined with the sonic anemometer/thermometer. The structure parameter is determined with equation 2, for several spatial separations. To check if the spatial separation are situated in the inertial sub range, in section 4.1 the temperature spectrum is shown. The temperature spectrum is calculated with the raw temperature data of the sonic anemometer/ thermometer by Fast Fourier Transform (FFT), with a segment length of 1024 s and a window of Welch.

From the spatial structure function and the spatial separation, the structure parameter of temperature is calculated. A disadvantage of using the sonic anemometer/ thermometer to determine the structure parameter is that the temperature fluctuations smaller than the path length,  $L$ , is not taken into account. To correct for these spectral losses, we use the correction of Hartogensis et al. (2002):

$$C_{T_{cor}}^2 = C_{T_m}^2 \cdot r^{\frac{2}{3}} \left[ \frac{2}{L^2} \int_0^L (L-x) \left( (r^2 + x^2)^{\frac{1}{3}} - x^{\frac{2}{3}} \right) dx \right]^{-1} \quad (15)$$

in which  $C_{T_{cor}}^2$  is the corrected and  $C_{T_m}^2$  is the measured structure parameter for temperature. The integration is done numerically.

### 3.2 The scintillometer

#### Set-up

An eXtra Large Aperture Scintillometer (XLAS) from Kipp & Zonen is set-up between the Cabauw Tower and the TV tower of IJsselstein (52°00'.72 N, 5°03'.23 E). The XLAS transmits a light beam with a near infrared wavelength of 880 nm. The aperture diameter has a size of 0.328 m. The distance between the two towers is 9.8 km. The transmitter is installed at the TV tower at 62.1 m height; the receiver is installed at the Cabauw tower at 61.7 m height. Consequently, the height of the optical path above the surface is then 59.9 m, which is the averaged height of the receiver and transmitter minus 2 meter for the earth's curvature at the middle of the path (Kohsiek, et al. 2002).

#### Data processing

The structure parameter of temperature is calculated from equation 5. For the temperature we used the 10 m temperature. The Bowen ratio is determined from the turbulent fluxes at 60 m, which are measured with the Licor and sonic anemometer/thermometer. The Bowen correction is not applied for Bowen ratios around -0.03 ( $-0.04 < \beta < -0.02$ ), because the Bowen correction becomes almost zero then, consequently the structure parameter of temperature would become extremely large.

We use the simplification of equation 6 to calculate  $A_T^2$  from the 10 m temperature and the surface pressure. The latter is measured at an automatic weather station site, 200 m southwest of the main tower. The instrument is a Paroscientific 1016B-01.



Figure 3 The receiver of the scintillometer at the Cabauw Tower at 61.7 m.

### 3.3 Data for MOST

For the use of MOST we need still some other data. The friction velocity is calculated for the various heights with the turbulent momentum flux obtained from the sonic anemometer/thermometer. The turbulent temperature scale and the Monin-Obukhov length are calculated with various combinations of the friction velocity and the turbulent temperature flux for the 60 m-, 100 m- and 180 m-level. For the first calculation (MOSTI) the friction velocity and the turbulent temperature flux at the respective level are used. The second calculation (MOSTs) makes use of the friction velocity at the respective level and the turbulent temperature flux at 3 m. We use also the friction velocity of the 60 m-, 100 m- and 180 m-level here, because in Cabauw a divergence in momentum flux is found, due to a difference in regional and local roughness (Beljaars, 1982). Consequently, the difference between the local and surface calculations corresponds with the use of respectively the local and surface turbulent temperature flux. All the used combinations are presented in Table 2. The temperature in the equation for determining the Monin-Obukhov length is taken from the 10 m level.

### 3.4 Selection of the data

This research considered only unstable conditions. Whether the atmosphere is unstable or not is height dependent. Therefore, the selection depends on the observed level. For every level only data is selected where the turbulent temperature flux of that level is positive.

The data is split in two groups for the 60 m-, 100 m- and 180 m-level. The first group contains data where the respective level is located above the surface layer, the early morning period, whereas the second group consists of data measured in the surface layer. The surface layer height ( $z_{SL}$ ) is determined as 10% of the boundary layer height ( $z_i$ ):  $z_{SL} = 0.1 \cdot z_i$ . The boundary layer height is determined from data of a wind profiler (LAP 3000) following Klein Baltink and Holtslag (1997) and Beyrich and Görsdorf (1995).

Table 2 The combinations of friction velocity and turbulent temperature flux to calculate the temperature scale and the Monin Obukhov Length.

	3 m	60 m		100 m		180 m	
		MOSTI	MOSTs	MOSTI	MOSTs	MOSTI	MOSTs
Friction velocity	$u_{*3}$	$u_{*60}$	$u_{*60}$	$u_{*100}$	$u_{*100}$	$u_{*180}$	$u_{*180}$
Turbulent temperature flux	$\overline{w'T'}_3$	$\overline{w'T'}_{60}$	$\overline{w'T'}_3$	$\overline{w'T'}_{100}$	$\overline{w'T'}_3$	$\overline{w'T'}_{180}$	$\overline{w'T'}_3$

## 4. Results and Discussion

### 4.1 Defining the inertial sub range

Before we investigate the behaviour of the structure parameter at the various heights, we determine for which time lag the relation of equation 2 is valid. In other words, we have to find out which wave numbers or frequencies are positioned in the inertial sub range, since the relation is only valid in this range. Equation 2 implies a  $-5/3$  power behaviour in the high frequency part of the spectrum. The temperature spectrum is calculated with a FFT from the raw temperature data of the sonic anemometer/ thermometer. So, the temperature is only corrected for wind speed and not for humidity and spectral losses at the high frequency area. Figure 4 shows the temperature spectrum for 3, 60, 100 and 180 m at 4 May 2008 1200 UTC averaged over 2 hours. All the four temperature spectra have a  $-5/3$  behaviour, however, the corresponding wave numbers ( $\kappa$ ) of the inertial sub range are not the same for the various heights. At 3 m the inertial sub range is from approximately  $0.2 \text{ m}^{-1}$  till  $0.6 \text{ m}^{-1}$ , which corresponds with a frequency ( $f$ ) between  $0.8 \text{ Hz}$  and  $2.3 \text{ Hz}$  ( $\kappa = f/\bar{U}$ ). This range is small in comparison with the ranges at the other heights. At 60 m the range varies from about  $0.03 \text{ m}^{-1}$  till  $0.2 \text{ m}^{-1}$  ( $0.15 \text{ Hz}$  till  $1.0 \text{ Hz}$ ), at 100 m the inertial sub range is between  $0.01 \text{ m}^{-1}$  and  $0.2 \text{ m}^{-1}$  ( $0.05 \text{ Hz}$  and  $1.06 \text{ Hz}$ ) and at 180 m from  $0.03 \text{ m}^{-1}$  till  $0.2 \text{ m}^{-1}$  ( $0.17 \text{ Hz}$  till  $1.12 \text{ Hz}$ ). The reason for the smaller range at 3 m is that the production of turbulence occurs at smaller scales. Note, that as a consequence of aliasing the values of the temperature spectrum are too high for high wave numbers. Based on the results of Figure 4, we choose the following time lags for 3 m: 0.5 s, 0.6 s, 0.7 s, 0.8 s and 0.9 s. For the other heights we used time lags of 1.6 s, 1.7 s, 1.8 s, 1.9 s and 2.0 s.

To ensure that these time lags are located in the inertial sub range, Figure 5 shows the time evolution for the structure parameter of temperature at the four heights. As can be seen, the structure parameter of temperature gives similar results for the various time lags at 60, 100 and 180 m, which indicate that the time lags are in the inertial sub range. The results for the five lags at 3 m differ more than the other locations; a difference around 5% between is found. However, this is to be expected for this low level; because due to the production of small eddies the inertial sub range is narrow for this location. From now on, we use a time lag of 0.7 s for calculating the  $C_T^2$  at 3 m, and a time lag of 1.8 s for the other levels.

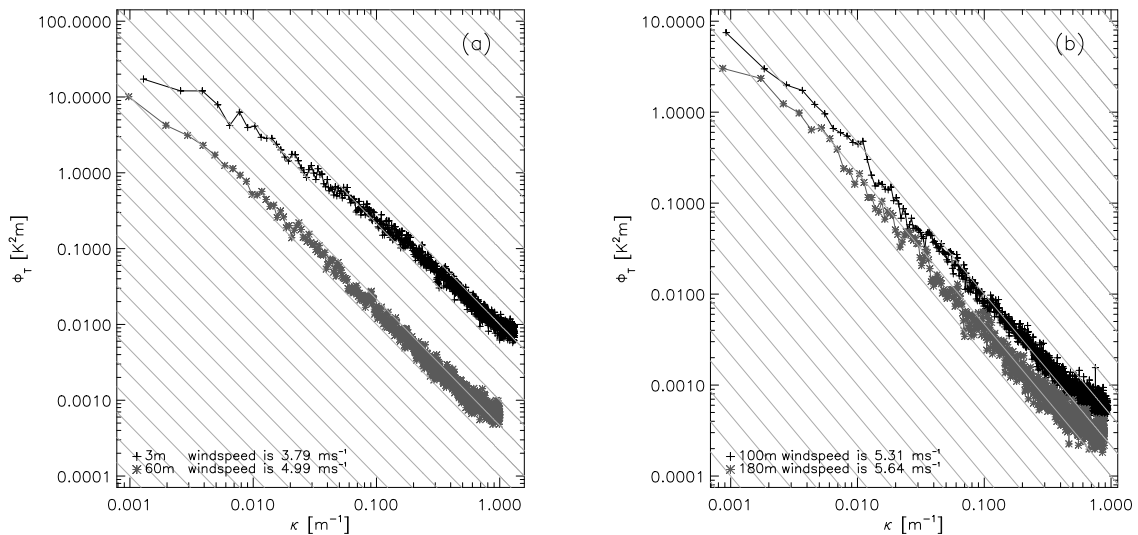


Figure 4 The temperature spectrum for (a) 3 and 60 m and (b) 100 and 180 m at 4 May 2008 1200 UTC. The dotted grey lines shows the  $-5/3$  behaviour.

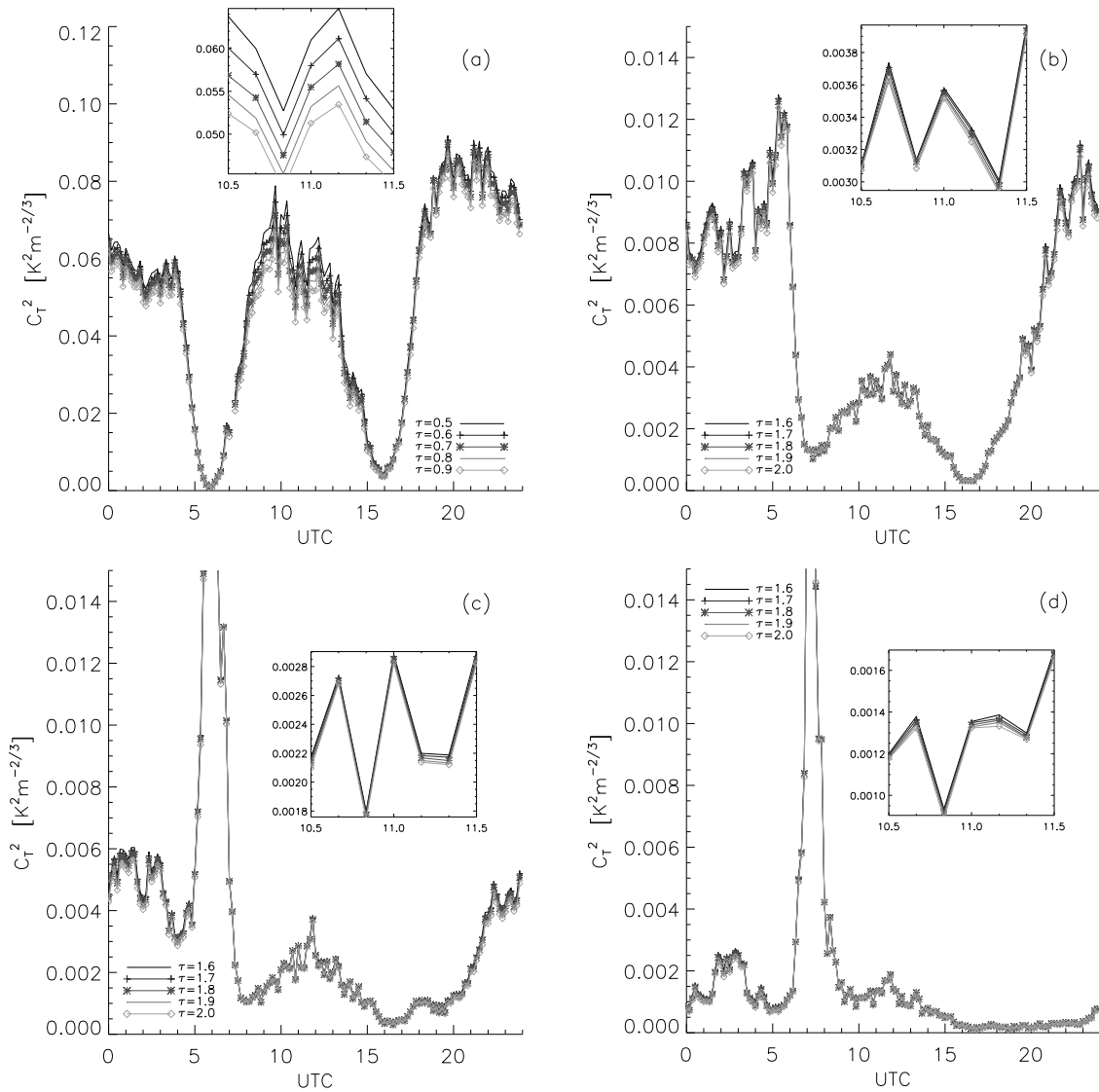


Figure 5 The time evolution of 10 minutes averaged corrected structure parameter of temperature at (a) 3 m, (b) 60 m, (c) 100 m and (d) 180 m averaged over the nine days. The small plots in the figures are an enlargement from 1030 till 1130 UTC.

As is shown in Figure 5, the structure parameter of temperature decreases with height. The values at 3 m are 10 times higher than for 60 m, which is in agreement with the theory. Something remarkable in the figure is that the structure parameter has an enormous peak at 100 and 180 m in the morning, before they reach their minimum. The peak can be observed at 60 m as well, however, this one is much smaller. The large values of  $C_T^2$  indicate a large amount of temperature fluctuations, which probably happened because the respective levels are situated in the entrainment zone. This is supported by the result that the peaks are not found at the same moment; the one at 180 m (0700 UTC) occurs about one hour later than those of 100 m (0600 UTC).

## 4.2 Boundary layer development: Boundary layer height and turbulent temperature fluxes

In a quasi-stationary boundary layer, temperature fluxes decrease linear with height and reach their minimum in the entrainment zone. In the surface layer, the fluxes are assumed to be constant with height, the fluxes differ not more than 10% of the surface flux. Consequently, we assume that the surface layer depth is the lowest 10 percent of the boundary layer. If the observations are located in the surface layer, the Monin Obukhov similarity theory is supposed to be valid, since the theory is defined for this layer. Since, the time evolution for boundary layer height and the turbulent temperature fluxes are important for the application of MOST, we analyse both parameters in this section.

The development of the boundary layer is quite comparable for the 9 days (figure not shown). The boundary layer starts growing around sunrise (0600 UTC). It reaches the 600 m level between 0930UTC and 1030UTC. Consequently, only in the early morning the 60 m level is not located in the surface layer. Then, the boundary layer is growing very fast: around 1000UTC and 1100UTC the boundary layer is 1000 m deep. At the end of the day, the boundary layer height reaches its maximum around 2000 m. Only at 5 May the boundary layer did not become deeper than 1800 m.

Figure 6 presents the time evolution of the four turbulent temperature fluxes averaged over the nine days. As expected the fluxes decrease with height in the morning period, when the surface layer is shallow. In the afternoon, we see that the values and the pattern of the fluxes at 60 m and 100 m are almost comparable: a constant flux layer. The 180 m flux shows a comparable pattern with the 60 m and 100 m as well, however the values of the 180 m flux are lower than the 60 m and 100 m, which we expected because the turbulent flux decreases with height outside the surface layer. Surprisingly, in the afternoon the 3 m flux is lower than the 60 m and 100 m flux, and more comparable with the 180 m flux.

The deviation of the 3 m flux can also be observed from Figure 7. The figure shows the 3 m flux together with the fluxes corrected for the flux divergence of 60 m, 100 m and 180 m level. Flux divergence correction is performed by adding the change of temperature storage in the air column below the measurement levels, assuming no advection. In this way the fluxes can be directly compared with each other. From the figure we observe that firstly the fluxes at the higher levels are comparable with each other, especially in the afternoon. Secondly, the 3 m flux deviates from the other fluxes. During the whole day, the values of the 3 m flux are almost 30 % lower than those of the other fluxes.

One possible reason for the differences between the turbulent temperature flux at 3 m and the other heights can be that the instrument at 3 m measures another footprint. If for instance the soil of the surroundings is drier than the soil around the tower, the latent heat flux measured at higher level is smaller than the one at 3 m and the sensible heat flux larger. However, further investigations are needed to give a complete explanation of the deviation of the 3 m flux.

Despite of the deviation of the 3 m turbulent heat flux, we choose to use the normal 3 m turbulent flux in the section 4.3, 4.4 and 4.5. Note, that the use of the measured 3 m flux could cause that the structure parameter of temperature calculated with the MOST and the turbulent temperature flux at 3 m underestimates the directly observed one at 60 m, 100 m or 180 m. Another, possibility is to use for instance the 60 m flux corrected for the flux divergence as an approximation for the 3 m turbulent heat flux, instead of the direct measured one. An advantage of the last method is that the footprint between the approximated 3 m and 60 m turbulent fluxes are the same. In section 4.6, we investigate the use of the flux divergence corrected 60 m flux.

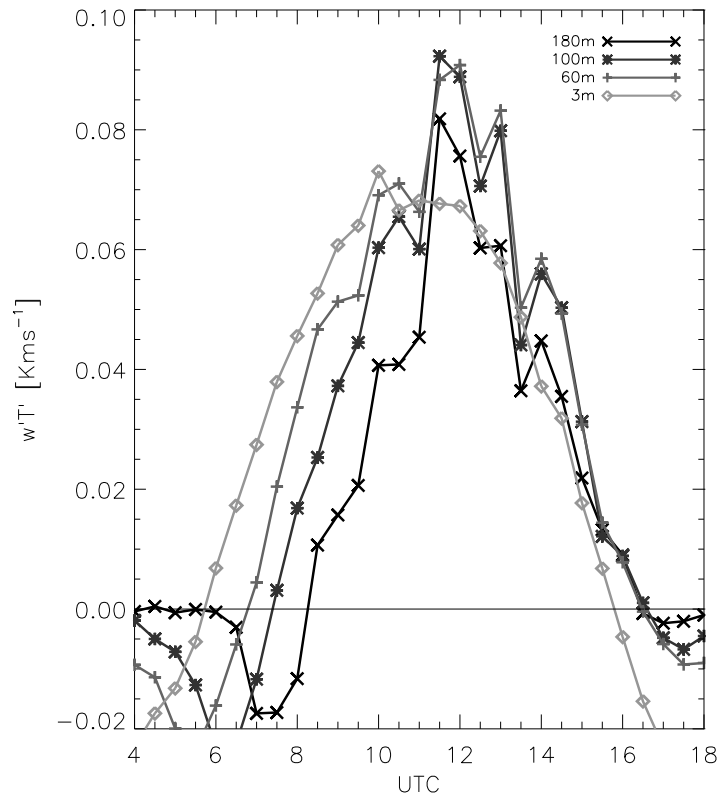


Figure 6 The time evolution averaged over the nine selected days of the turbulent temperature flux at 3 m( $\diamond$ ) 60 m (+), 100 m (\*) and 180 m( $\times$ ).

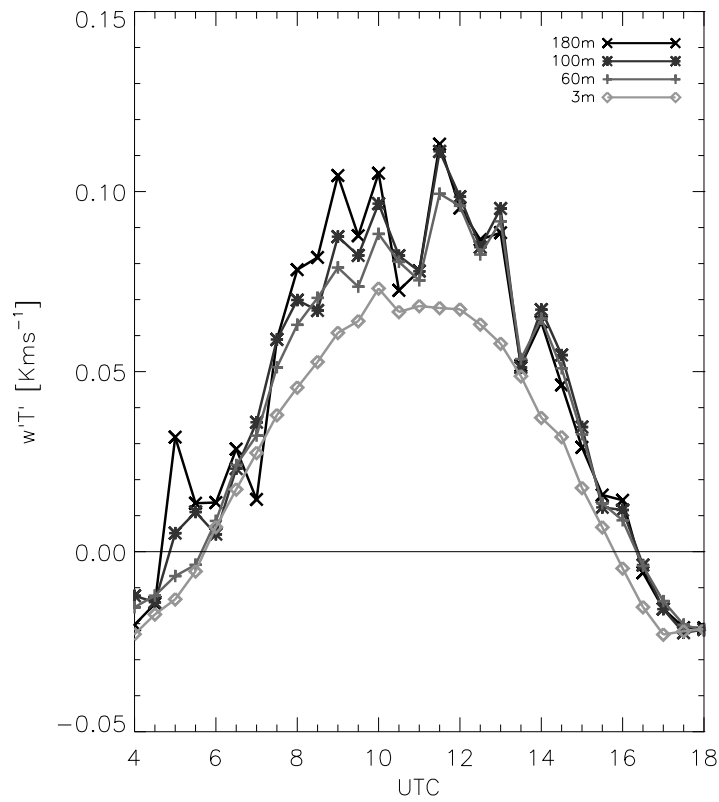


Figure 7 The time evolution averaged over the nine selected days of the turbulent temperature flux at 3 m ( $\diamond$ ), and the for flux divergence corrected turbulent flux at 60 m (+), 100 m (\*) and 180 m ( $\times$ ).

#### 4.3 The structure parameter of temperature at 3 m

In this section, we investigate if MOST is valid for our dataset and which of the proposed equations gives the best result. We will do this by analysing the 3 m observations, since this level is located in the surface layer the entire day. Figure 8 shows the observed similarity relation between  $\frac{z}{L_{Ob}}$  and  $\frac{C_T^2 \cdot z^{2/3}}{T_*^2}$

for 3 m and the published relationships that are mentioned before. As can be observed, the data show a similar pattern as the proposed equations, which give a first indication that for 3 m MOST is reliable. The similarity equation proposed by Hill et al. (1992) has the best fit through the data especially under near neutral conditions. It is not surprising that this equation fits quite well here, because the equation is an adjustment of those of Wyngaard (1973) to better fit the near neutral data. The equation of Hill et al. is used

from now on. For  $-\frac{z}{L_{Ob}} < 0.03$  more scatter is found. In this region, the observed data show larger values

for the  $\frac{C_T^2 \cdot z^{2/3}}{T_*^2}$  in comparison with the proposed functions. The corresponding times of these

observations are in the late afternoon (light grey points), when the turbulent temperature flux is small and still some temperature fluctuations are observed. The small fluxes cause that the temperature scale becomes small as well, whereas the structure parameter will not become zero due to the observed temperature

fluctuations, which caused the high-observed values for  $\frac{C_T^2 \cdot z^{2/3}}{T_*^2}$ .

In Figure 9 the variation in time, averaged over 9 days, of the structure parameter of temperature measured with the sonic anemometer/ thermometer and calculated from MOST are plotted, as well as the 3 m turbulent temperature flux. The bold part of the lines represents the unstable conditions, where the turbulent temperature flux is larger than zero. The equation of Hill et al. (2002) gives almost the same results as observed from the sonic anemometer/ thermometer during daytime. When the turbulent flux is about zero (neutral conditions) around 0600 UTC and 1600 UTC, the temperature fluctuations are small. Consequently, both structure parameters reach their minimum.

Figure 10 presents the 3 m observed data of the structure parameter of temperature observed from the sonic anemometer/ thermometer against the one computed from MOST. There is a good correlation between the observed and computed values for the structure parameter: the correlation coefficient is 0.93. The best fit through the data has the form of:  $C_{T_{MOST}}^2 = 0.89 \cdot C_{T_{sonic}}^2 + 2.7 \cdot 10^{-3}$ . Hence, the values of the structure parameter from MOST slightly underestimate the measured values from the sonic anemometer/ thermometer.

Altogether, the three figures shows that the results of the structure parameter of temperature calculated with MOST are comparable with those directly obtained from the sonic anemometer/ thermometer at 3 m. This indicates that MOST is a good tool to estimate the surface sensible heat fluxes from the structure parameter of temperature close to the surface.

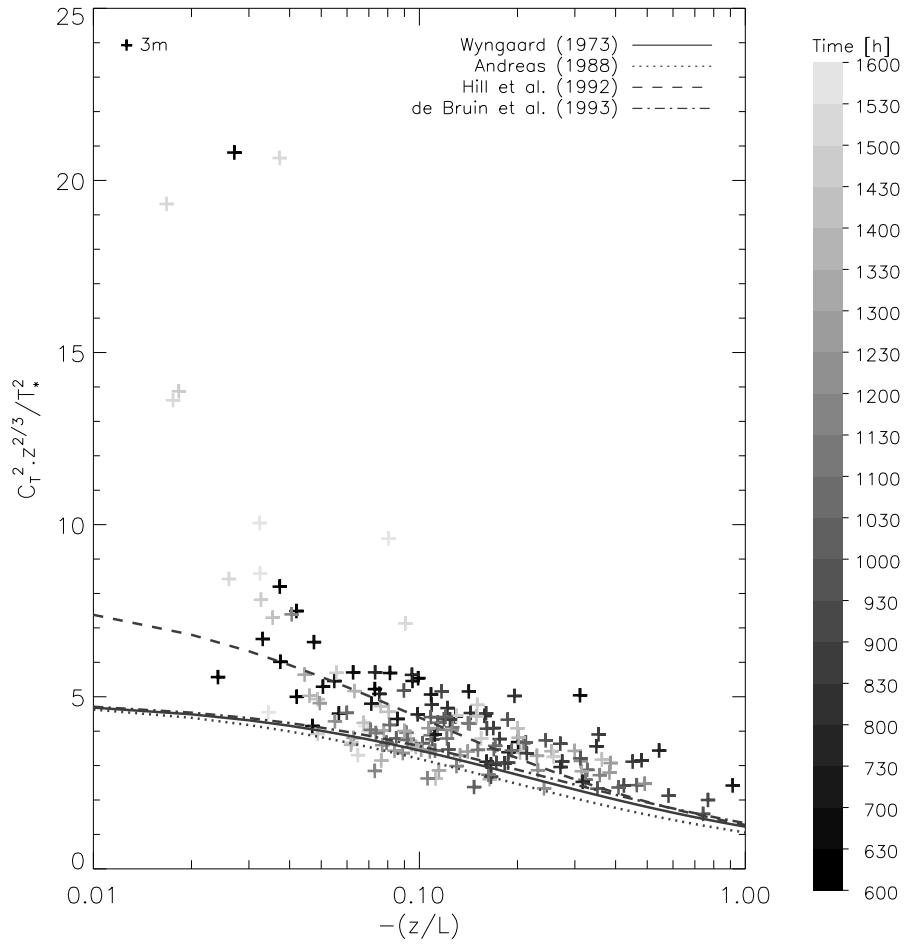


Figure 8 The 3 m values of the similarity relation obtained from the turbulent temperature flux and the friction velocity at 3 m (+) and the four proposed similarity equations (lines) under unstable conditions ( $w'T_{3m}' > 0$ ). The colour indicates the time of the observation in UTC. Values for  $\frac{C_T^2 \cdot z^{2/3}}{T_*^2}$  higher than 25 are not taken into account.

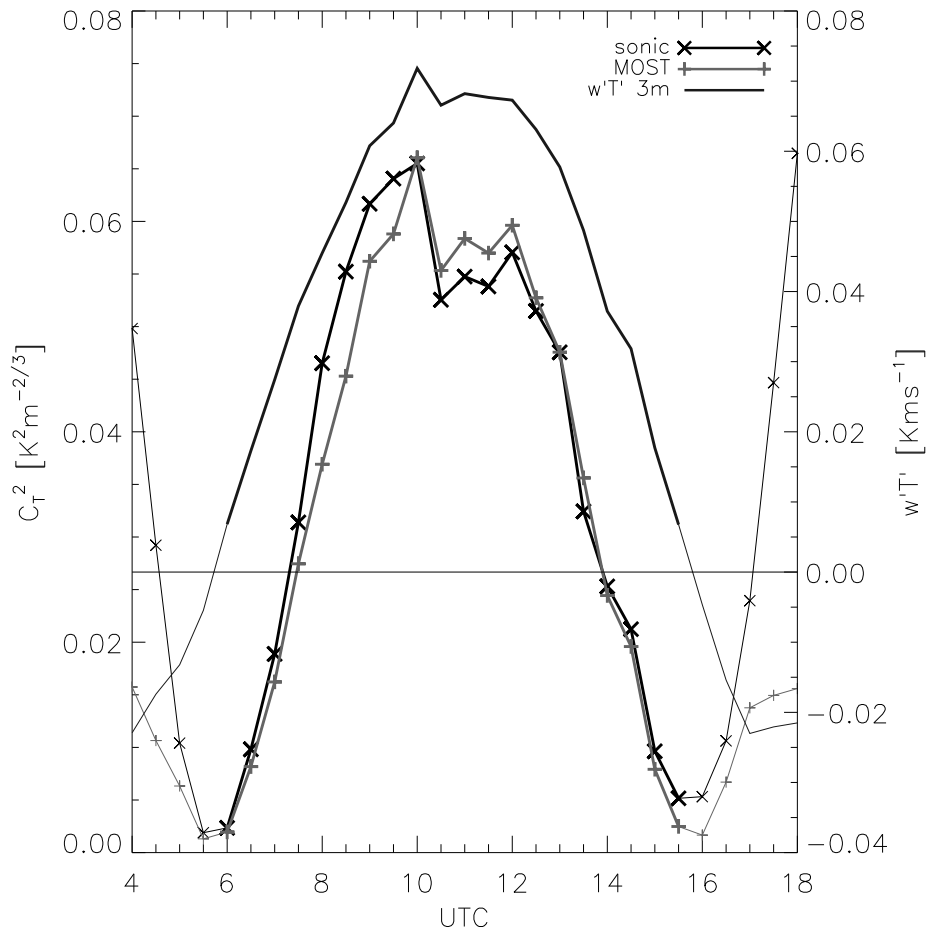


Figure 9 The time evolution averaged over the nine selected days of the structure parameter of temperature observed from the sonic anemometer /thermometer ( $\times$ ), and calculated with MOST (+) of Hill, , and the turbulent temperature flux at 3 m. Bold are the unstable conditions ( $w'T'_{3m} > 0$ ) Note that the structure parameter and the flux have different y-axes left and right, respectively.

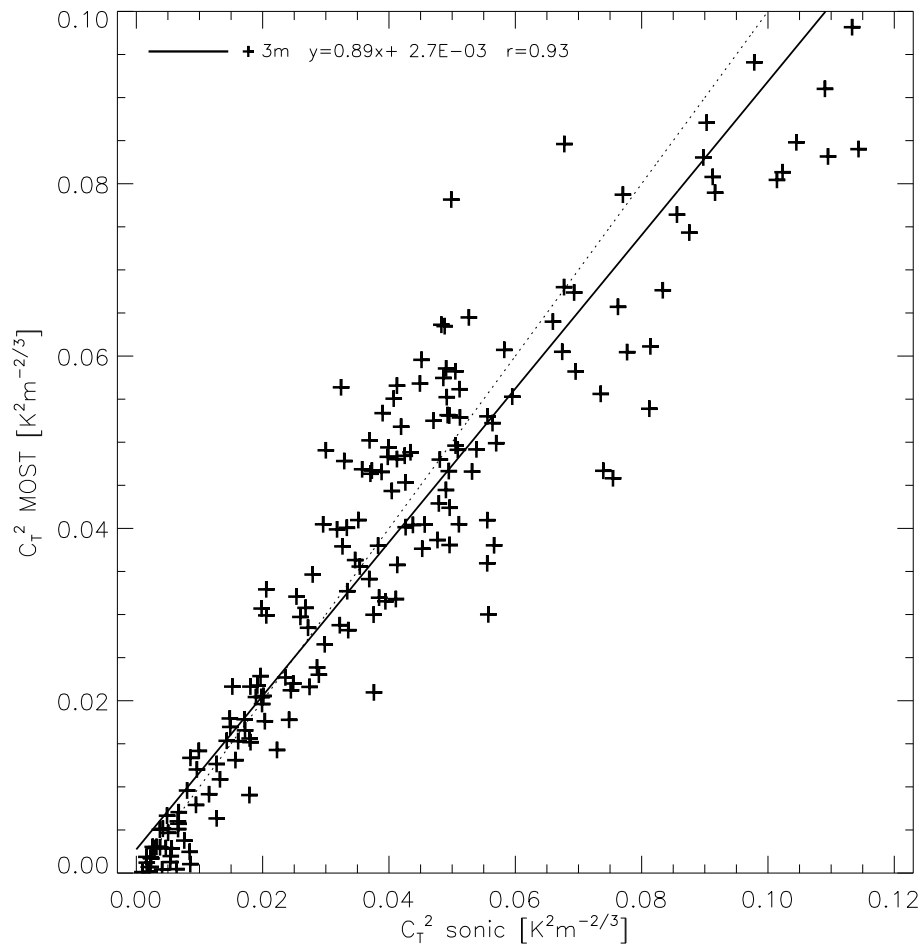


Figure 10 The structure parameter of temperature observed from the sonic anemometer/ thermometer against the structure parameter calculated with MOST for unstable conditions at 3 m. The solid line is the best fit through the data. The dotted line represents the 1:1-line.

#### 4.4 The structure parameter of temperature at 60 m

In Figure 11 the time evolution of the 60 m structure parameter of temperature measured with the sonic anemometer/ thermometer, the scintillometer and calculated from MOST are given, as well as the turbulent temperature flux at 3 m and 60 m. The measured structure parameter from the sonic anemometer/ thermometer and the scintillometer are quite comparable. The minima of both structure parameters of temperature are on the same time, at 0700 UTC in the morning and 1600 UTC in the afternoon. In the morning these minima are found at the same time when the turbulent temperature flux at 60 m is around zero, which is almost 2 hours after the moment when the turbulent temperature flux at 3 m goes through zero. Minimal temperature fluctuations under neutral conditions cause a temperature flux of around zero and a minimum in the structure parameter of temperature as well. Thus, in the morning transition period, the pattern of the structure parameter at 60 m follows the pattern of the local turbulent temperature flux at 60 m. The peak in the structure parameter at 0530 UTC corresponds with the minimum turbulent temperature flux, which indicates that the maximum in the structure parameter is found because the entrainment layer is around the 60 m-level, as mentioned before.

One difference between the observations from the scintillometer and the sonic anemometer is that the first one gives smoother results, which is probably caused by the difference in footprint and path averaging. The observations of sonic anemometer/ thermometer are local measurements, whereas the scintillometer measures along a path. Consequently, the sonic anemometer/thermometer is more sensitive to temperature fluctuation of one local eddy, which caused a larger variation in the signal. The correlation coefficient between the data of the sonic anemometer/ thermometer and the scintillometer is 0.80.

Although, the minimum of the structure parameter at 60 m occurs at the same time as when the turbulent flux at 60 m becomes positive, it does not say anything about the behaviour of the structure parameter in relation to the temperature flux during the day. Therefore, the structure parameter of temperature calculated with MOST is plotted in Figure 11 as well. Note that the structure parameter is calculated from the temperature flux at 60 m and the friction velocity at 60 m (MOST1) and from the temperature flux at 3 m combined with the friction velocity at 60 m (MOSTs).

The structure parameter of temperature calculated from the temperature flux at 60 m shows a variable pattern, whereas those calculated at 3 m is much smoother. At 3 m the eddies are smaller than at 60 m and much more eddies pass the sensor during the averaging time resulting in statistically more stable values. As expected, the structure parameter calculated from the 60 m turbulent temperature flux reaches its minimum around 0700 UTC, at the same moment as those directly observed. The structure parameter calculated from the 3 m temperature flux reaches its minimum earlier in time. However, the values of the structure parameter calculated with MOST1 are lower in comparison to the one measured with the sonic anemometer/ thermometer, and those with MOSTs are more compatible. In the afternoon, the opposite is observed: the structure parameter calculated from the 60 m temperature flux is quite similar with the measured one from the sonic anemometer/ thermometer. The results calculated from the 3 m level are smaller. This is an unexpected observation and does not follow one of the two theoretical concepts. Since, we expect that in the afternoon, when the 60 m level is located in the surface layer, MOST is valid. Consequently, the structure parameter calculated with the 3 m temperature flux has to be the same as the one calculated at 60 m and the observed ones. The reason for the small values of the structure parameter measured with the 3 m flux is that the 3 m flux is smaller as well, as mentioned in section 4.2.

The conspicuous results found in Figure 11 are confirmed with those from Figure 12. Figure 12 shows the observed structure parameter of temperature against those calculated with MOST. Two different groups can be distinguished: dark colours indicate times when the 60 m level is outside the surface layer (early

morning period), while light colours are moments where 60 m is situated in the surface layer (the afternoon). For the last period MOST is supposed to be valid.

Considering the data during the whole day, we perceive that the data calculated from MOSTl correlates better than those of MOSTs with the observed data of the sonic anemometer/ thermometer. The correlation coefficient of the first is 0.81, whereas the second has a correlation coefficient of 0.71. In both cases, the correlation is much worse than the correlation between the observed and measured structure parameter at 3 m. The best fit through the data calculated with the 60 m temperature flux has the form of  $C_{T\ MOSTl}^2 = 1.14 \cdot C_{T\ sonic}^2 - 6.5 \cdot 10^{-4}$ . The equation for those calculated with the 3 m temperature flux is as follows:  $C_{T\ MOSTs}^2 = 0.77 \cdot C_{T\ sonic}^2 - 2.9 \cdot 10^{-5}$ . The first one underestimate the structure parameter of temperature measured by the sonic in particular when small values are observed (the morning period). The second one on the contrary underestimates especially higher values, which already was observed in Figure 11.

In the second place the data outside the surface layer will be discussed. On average, for these days 60 m is situated outside the surface layer till about 1000 UTC. From Figure 11, one can already observe that at this time the use of the 3 m turbulent temperature flux gives reliable results, while the use of the 60 m temperature flux underestimate the structure parameter. The linear fits through the data in Figure 12 shows just the same. Moreover, the correlation between the calculated and measured data is 0.80 in the case of using the 3 m turbulent temperature flux; whereas the correlation coefficient using the 60 m flux is much lower (0.66).

Lastly, for the data inside the surface layer MOSTl show almost a 1:1-relation with the observed data. On the other hand, MOSTs underestimated the structure parameter of temperature. Furthermore, a higher correlation between the structure parameter calculated from the 60 m turbulent temperature flux and the one of the sonic anemometer/ thermometer is found than between the one measured at 3 m. The first one has a correlation coefficient of 0.84 in comparison with 0.72.

The similarity relation between the stability parameter  $\frac{z}{L_{Ob}}$  and the dimensionless group:  $\frac{C_T^2 \cdot z^{2/3}}{T_*^2}$

for the 60 m level is presented in Figure 13. For the calculation of the Monin Obukhov length and the temperature scale the combinations of the turbulent temperature flux and the friction velocity according to Table 2 are used. Because the stability parameter is height dependent, one can observe that the stability parameter is larger for 60 m than for 3 m (Figure 8). During unstable cases with  $-\frac{z}{L_{Ob}} > 1$ , most of the data follows the proposed equations. Only some data points in the early morning (from 0600 UTC till 0900 UTC) calculated with the temperature flux at 60 m and the friction velocity at 60 m are larger. A reason for the larger values is that the turbulent temperature flux at 60 m has low values (Figure 11), which result in small values for the temperature scale.

However, under more neutral conditions the observed data deviates more from the equations, especially the data calculated with the 3 m turbulent flux. In general, the times when these data points are observed are in the afternoon. As already shown in Figure 6, in the afternoon low values for the turbulent temperature flux at 3 m are found, which caused the overestimation in the temperature scale and consequently in the dimensionless group as well.

Overall, the data do not confirm one of the two theoretical concepts. The transition between stable and unstable conditions of the observed structure parameter of temperature at 60 m is comparable with the transition measured by the 60 m turbulent flux. However, in the rest of the morning period the observed

structure parameter follows the one calculated with the 3 m temperature. During the afternoon, if the 60 m level is situated in the surface layer, the observations do not follow MOST. Since, the turbulent temperature flux at 60 m is larger than the one at 3 m and varies more than 10%, the  $C_T^2$  calculated with the temperature flux at 60 m correlates better than the 3 m flux. In general, the structure parameter of temperature defined by MOST underestimates the one measured from the sonic anemometer/ thermometer. To gain more insight into the unexpected results of 60 m and because sonic anemometers/ thermometers are installed at 100 m and 180 m as well, these data is discussed and compared with the data at 60 m in the next section.

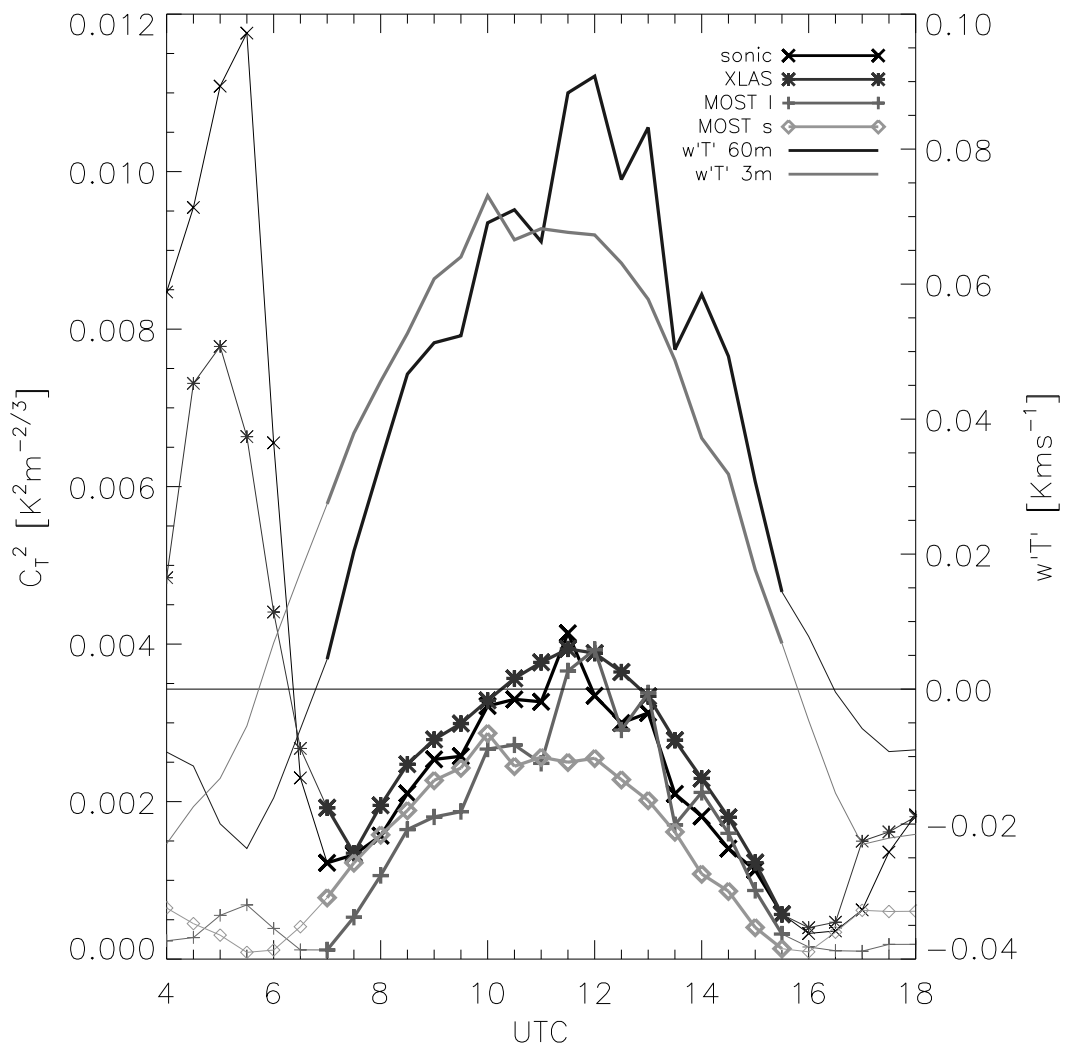


Figure 11 The time evolution averaged over the nine selected days of  $C_T^2$  observed from the sonic anemometer/ thermometer at 60 m ( $\times$ ), and the scintillometer at 60 m ( $*$ ), calculated with MOST using combination l (+) and s ( $\diamond$ ) from Table 2. As well as the turbulent temperature flux at 3 m (grey) and 60 m (black). Bold are the unstable conditions ( $w'T'_{60m} > 0$ ).

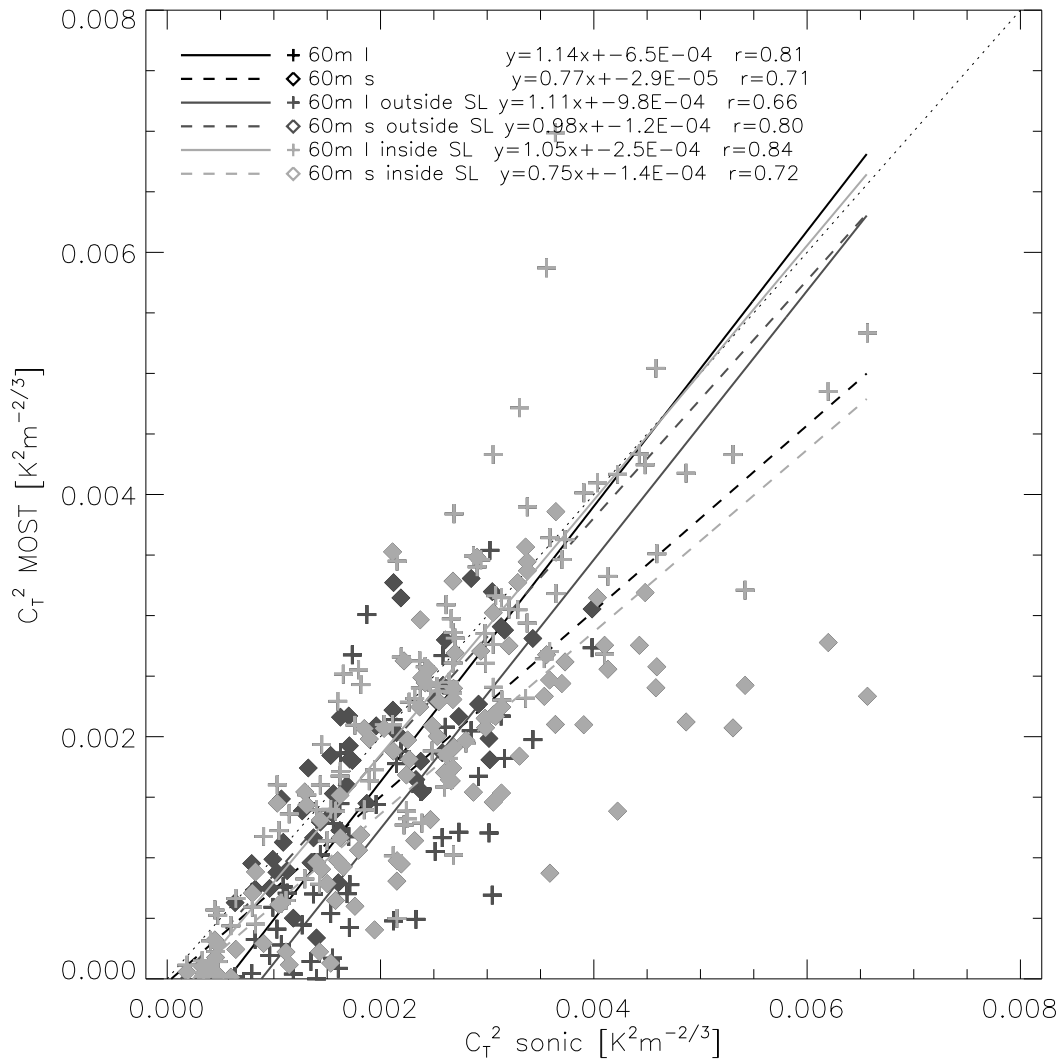


Figure 12 The structure parameter of temperature at 60 m of the sonic anemometer against those of MOST, calculated with using combination a (+) and b (◆) from Table 2 under unstable conditions ( $w'T'_{60m} > 0$ ). Dark colours represent data points where 60 m is situated outside the surface layer, whereas light colours represent data inside the surface layer. The lines are the corresponding best fits through the data.

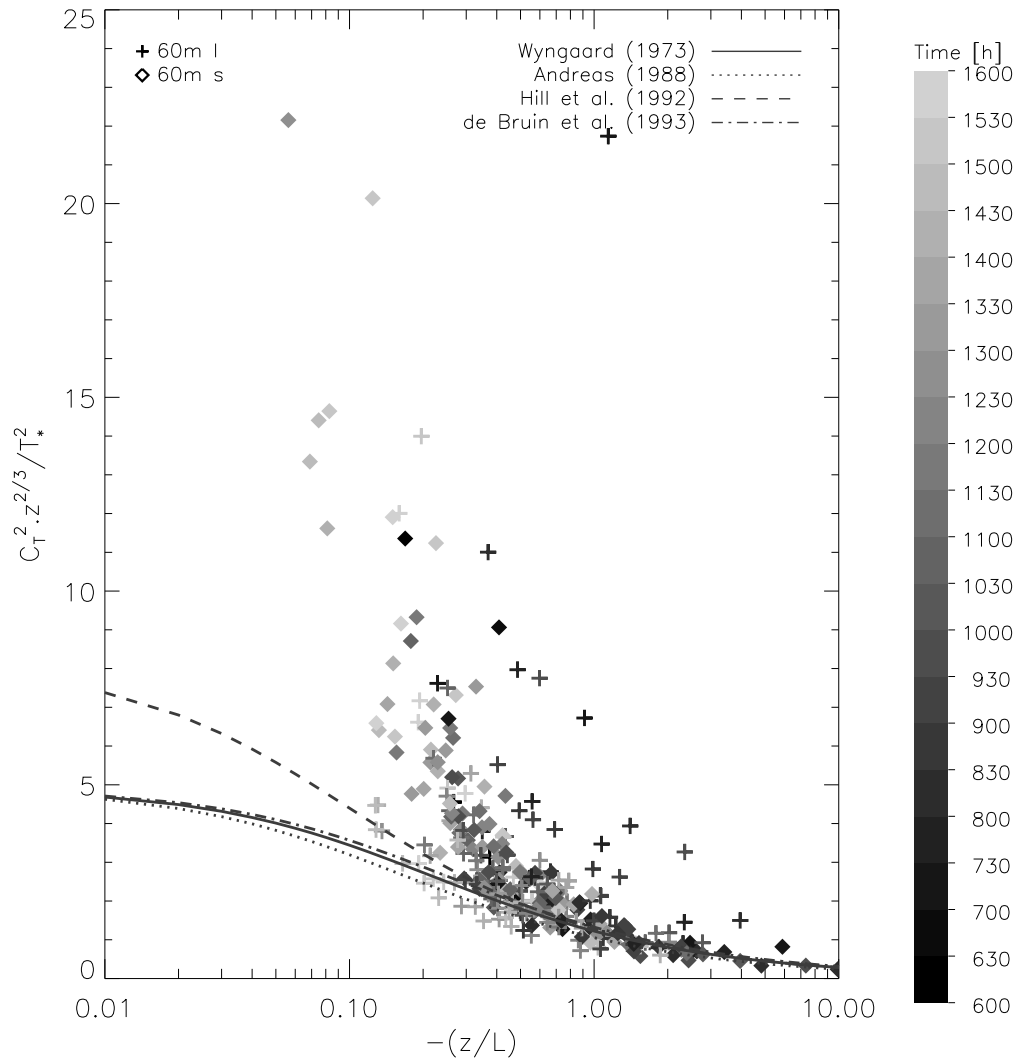


Figure 13 As in Figure 8, but now the data is obtained from the turbulent temperature flux and the friction velocity both at 60 m (+), and from the turbulent temperature flux at 3 m with the friction velocity at 60 m (◆), respectively combination a and b from Table 2. Note that for the structure parameter the data of the sonic anemometer/ thermometer is used.

#### 4.5 The structure parameter of temperature at the other heights

Figure 14 shows the time-evolution for the structure parameter of temperature and the turbulent temperature flux for 100 m (a) and 180 m (b). At the two levels, the measured structure parameter of temperature from the sonic anemometer/ thermometer has a peak in the morning at the same time when the turbulent temperature flux of the respective level has a minimum at these times: the respective levels are located in the entrainment zone. The time when the 100 m flux is around zero a minimum of  $C_T^2$  can be found, which is similar with the results from the 60 m level (Figure 11). For 180 m the structure parameter minimum is observed somewhat later than when the flux is around zero. During the morning, the structure parameter calculated from MOST underestimates the observed one for both levels. Using the 3 m turbulent flux in MOST gives more comparable results with the measured one, than using the local turbulent flux. In the afternoon the turbulent temperature flux at 100 m is larger compared to the 3 m flux, whereas the 180 m flux has similar values with the one at 3 m. Consequently, at 100 m the structure parameter of temperature calculated with MOSTI is higher and is in better agreement with the observed values than MOSTs, whereas at 180 m the structure parameter obtained with MOSTI and MOSTs has almost the same values. However, both calculations for the two heights underestimate the observed structure parameter of temperature. Comparing the 60 m, 100 m and 180 m level with each other, it seems that the underestimation becomes larger by increasing height.

In Figure 15 the observed structure parameter against the two calculated from MOST are plotted. In the figure, a distinction is made between the data points inside and outside the surface layer. On average, the 100 m and 180 m level are located in the surface layer from respectively about 1030 UTC and about 1300 UTC. However, at 3 May 2008 the 180 m level is outside the surface layer the whole day. From Figure 15a can be concluded that the results of 100 m-level has the same pattern as those of 60 m. Firstly, if all the data are taken into account higher correlation is found between MOSTI ( $r=0.76$ ) and the sonic anemometer/ thermometer than between MOSTs ( $r=0.54$ ). Secondly during the morning, when 100 m is not located in the surface layer, the use of turbulent temperature flux at 3 m provide higher correlation ( $r=0.73$ ). Thirdly, in the afternoon the calculations with the 100 m flux (MOSTI) correlate better with the sonic anemometer thermometer data.

At 180 m the same pattern is found for all the data and the afternoon, however, in the morning period a very small correlation ( $r=0.24$ ) is found for the data from MOSTs and the sonic anemometer/ thermometer, while at the other heights MOSTs has the highest correlation if the level is outside the surface layer. Analysing the figure, the data outside the surface layer calculated with the 3 m turbulent temperature flux can be split in two groups. One scatter cloud is around the  $x=y$  line, the other one consist of a few data points with high values of the sonic and low values for MOST. The last group cause the correlation to be low. These data correspond with the early morning period, where the structure parameter of temperature observed from the sonic anemometer does not have reached their minimum yet, while the turbulent temperature flux is already positive (see also Figure 14b).

The best fits through the data in Figure 8, Figure 12 and Figure 15 indicate that by increasing the height the underestimation of the structure parameter of temperature calculated by MOST in comparison with the one observed by the sonic anemometer/ thermometer becomes larger. Further, in general, the correlation coefficient between observed and calculated  $C_T^2$  decreases with height, except for some correlation coefficients at 180 m.

Figure 16 presents the relation between  $\frac{z}{L_{Ob}}$  and  $\frac{C_T^2 \cdot z^{2/3}}{T_*^2}$  for 100 m and 180 m, respectively Figure

16a and 16b. Comparing Figure 16 with Figure 10 and 13, one can observe that by increasing the height, the data deviates more from the proposed equations. For 100 m and 180 m the published similarity relations fits through the data only under very unstable conditions, as observed for the 60 m too. In the morning period (dark colours) the data from the temperature flux at the respective level (+) overestimate the dimensionless group:  $\frac{C_T^2 \cdot z^{2/3}}{T_*^2}$  in comparison with values of the proposed equations. Whereas in the afternoon (light colours) the data calculated from the 3 m temperature ( $\blacklozenge$ ) flux varies more from the equations.

Altogether, comparing the data of the various heights, we observe that by an increase of height (a) the correlation between the calculated and the measured  $CT_2$  decreases, (b) MOST underestimate the observed values more and (c) the observed data deviates more from the proposed equations for the similarity relations between  $\frac{z}{L_{Ob}}$  and  $\frac{C_T^2 \cdot z^{2/3}}{T_*^2}$ . This indicates that MOST is maybe not the right tool to obtain the turbulent temperature flux from the structure parameter at these levels. Probably, processes at the surface are not the only one that dominates turbulence at higher levels. Consequently, another parameter, such as the boundary layer height, can be of interest to take into account in the dimensional analysis. Therefore, in further research, it would be interesting to investigate whether for instance local-free-convection scaling as is described by Wyngaard (1973) can be used to determine the turbulent fluxes from the structure parameter of temperature.

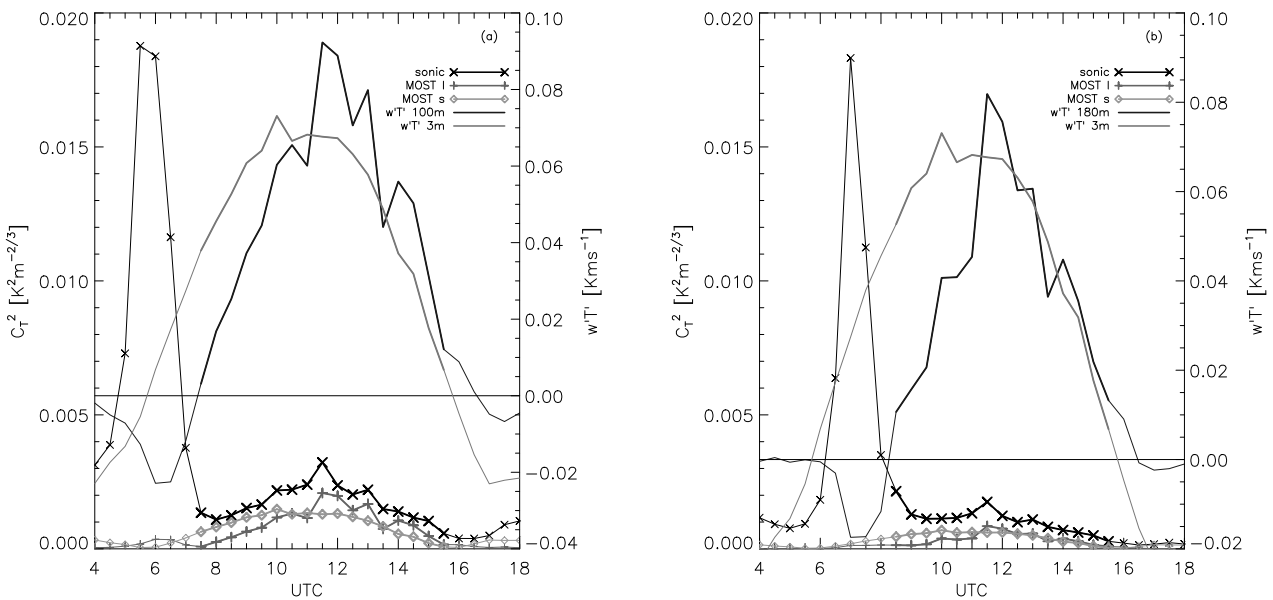


Figure 14 As in Figure 9, but now for (a) 100 m and (b) 180 m.

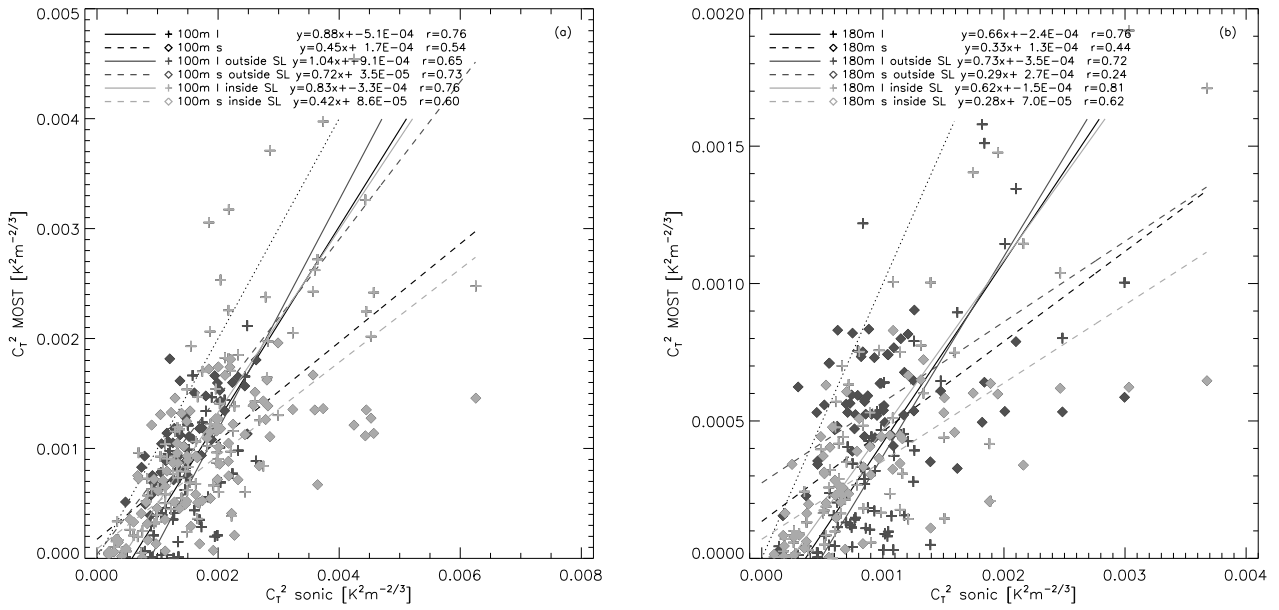


Figure 15 As in Figure 10, but now for (a) 100 m and (b) 180 m.

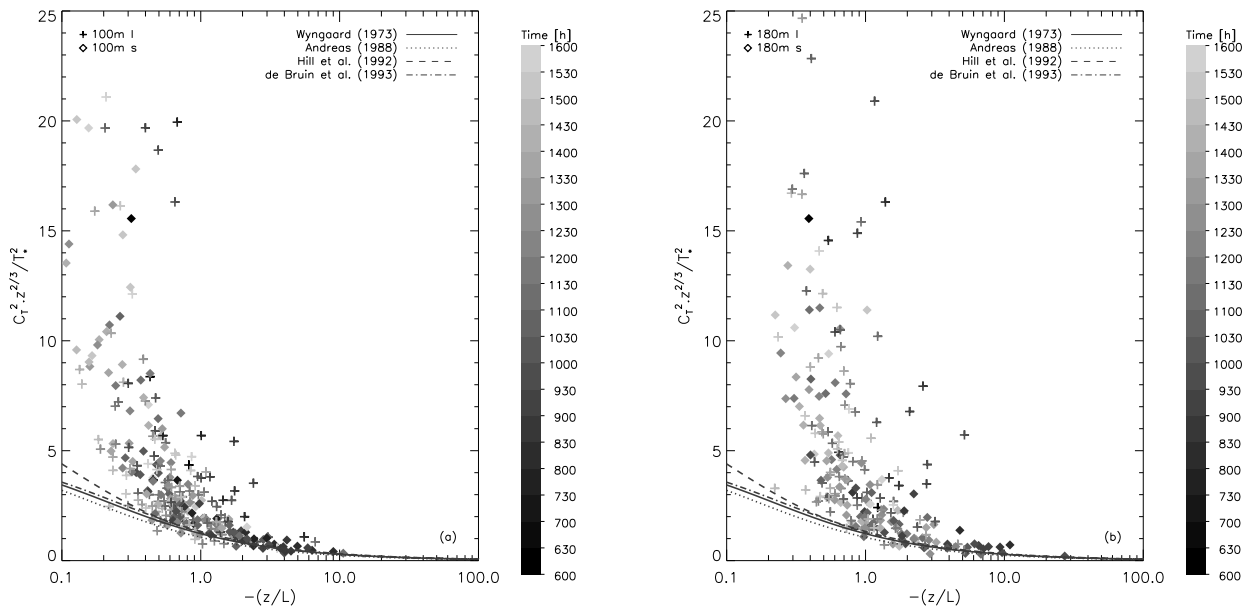


Figure 16 As in Figure 11, but now for (a) 100 m and (b) 180 m.

#### 4.6 The structure parameter of temperature at 60 m revised

In section 4.2 we observed that the 3 m flux shows a different pattern than the other levels. In the sections above, we saw that using this flux influences the results directly and make the results difficult to interpret. As mentioned before, we can also use the 60 m flux corrected for the flux divergence as the 3 m flux, instead of using the observed 3 m turbulent temperature flux. In this section, we discuss the results of using the for flux divergence corrected 60 m flux. This flux is called the 60 m base surface temperature flux.

Figure 17 shows the same results as Figure 11, but now with using the flux divergence corrected 60 m flux as the surface flux. Now, we observe a clear constant flux layer in the afternoon. For the moment of transition between the stable cases during the night and the unstable cases during the day, we observe the same results as from Figure 11. The minimum in the structure parameter calculated with the turbulent temperature 60 m flux is at the same moment as observed with the sonic anemometer/ thermometer. If the 60 m based surface temperature flux is used, the minimum is observed one hour earlier, at the same moment as the 60 m based surface flux becomes positive.

Furthermore, the results differ from Figure 11. In the morning period, neither of the two concepts gives the correct answer. The values for the direct measured structure parameter of temperature lies between those calculated with MOST1 and those calculated MOSTs. The first one overestimates, and the second one underestimate the directly measured values. However, in the afternoon the data show more expected results than in Figure 11. Due to the constant flux layer, the structure parameter obtained from the two concepts give comparable results with the direct measured structure parameter of temperature.

In Figure 18 the structure parameter of temperature measured with the sonic is plotted against the two obtained from MOST theory according to the two concepts. We observe that during the whole day, the correlation between the direct measured  $C_T^2$  and those of MOST, is comparable for both concepts, respectively 82% and 83% for MOST1 and MOSTs. So, using the flux divergence corrected 60 m flux instead of the 3 m flux as the surface flux improves the results for MOSTs. Despite of the comparable results for the correlation coefficient, a difference is found between the values of the structure parameter. In general, using structure parameter calculated from the local flux overestimated the measured one, whereas using the one from the surface flux gives lower values, as also observed in Figure 17.

In the morning period when the 60 m level lies outside the surface layer, the correlation is better if the local flux (0.78) is used than the surface flux (0.72). However, the difference in the correlation coefficient is smaller than when using the 60 m based surface temperature flux. Inside the surface layer; we observe higher correlation coefficient for both methods. Here the use of the 60 m turbulent heat flux gives less scatter than the surface turbulent heat flux, the correlation coefficient is respectively 0.83 and 0.87. Because, the difference in the correlation coefficients is not that big anymore, it would be interesting to analyse this data with more advanced statistical tools or for more days.

Using the 60 m flux corrected for flux divergence as surface flux gives more comprehensible results. However, still neither of the two concepts is the final answer. In the morning period, the measured structure parameter lies even between the two structure parameter obtained from the two concepts. Therefore, it would be interesting to investigate this also for the other levels; however, this is not done here due to lack of time in the project. Further, firstly to get a better understanding of the behaviour of the structure parameter of temperature and secondly to know which of the two models gives the best result, we recommend investigating the structure parameter at higher levels with a Large Eddy Simulation (LES). This might shed light on the importance of different processes that act on the structure parameter.

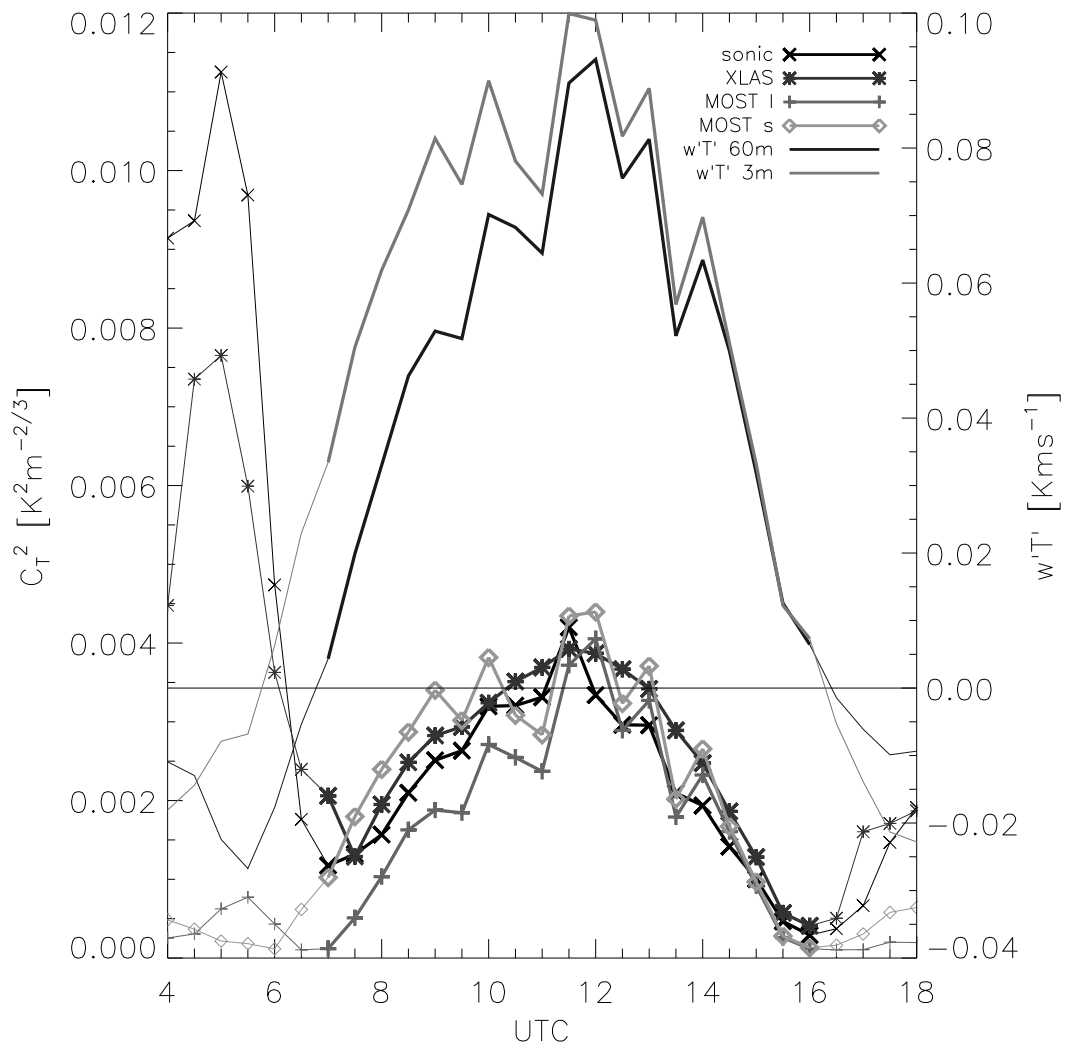


Figure 17 As in Figure 11 but now with using the for flux divergence corrected 60 m turbulent heat flux as the turbulent heat flux at 3 m. Only the days from 4 May to 11 May are plotted.

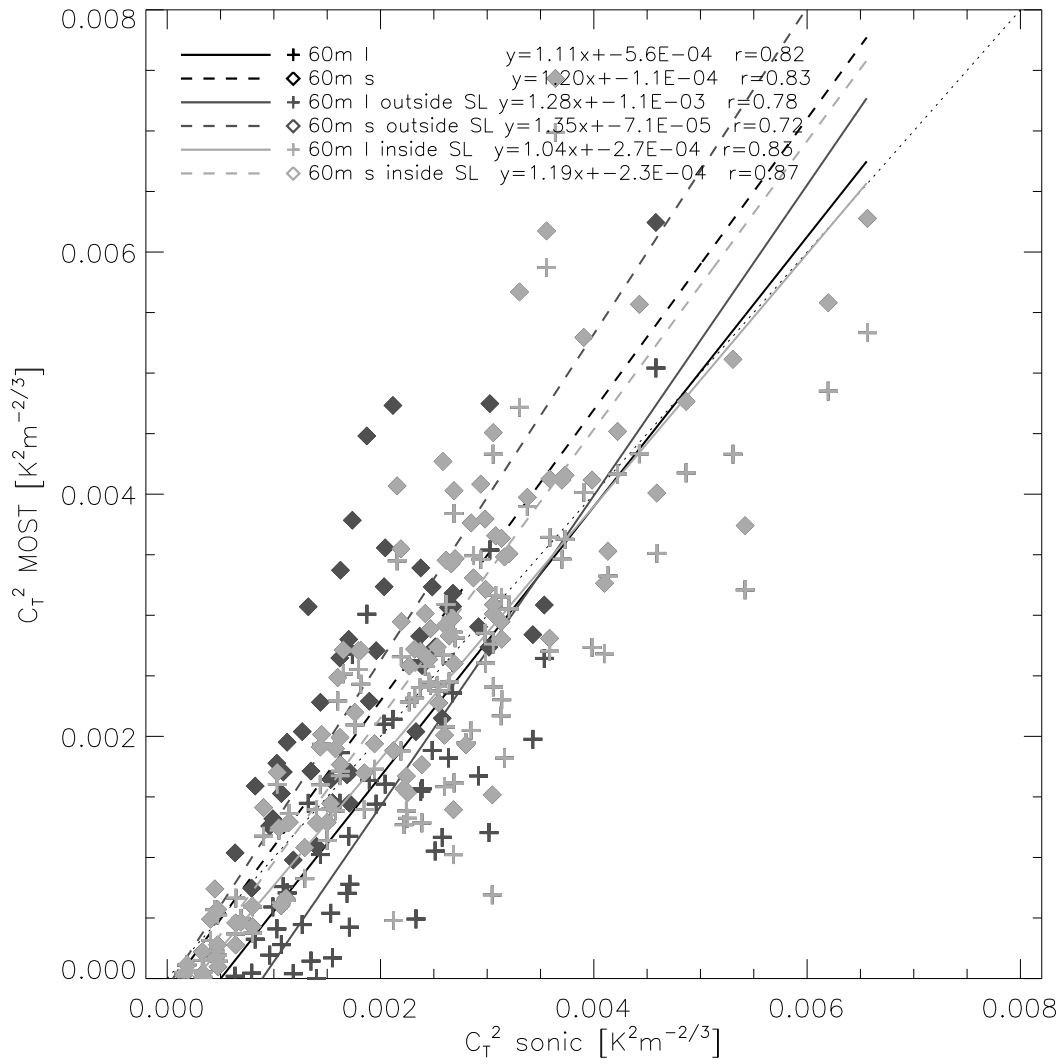


Figure 18 As in Figure 12 but now with using the for flux divergence corrected 60 m turbulent heat flux as the turbulent heat flux at 3 m. Only the days from 4 May to 11 May are plotted.

## 5. Conclusions and Recommendations

In order to investigate in which way the turbulent surface sensible heat flux can be estimated from  $C_T^2$  determined from a scintillometer at 60 m, two different theoretical concepts were compared. In the first concept one assumed that the structure parameter of 60 m has to be scaled with the 60 m flux themselves, whereas in the second one supposed that the surface turbulent flux have to be used. To ensure that the footprints of  $C_T^2$  and  $\overline{w'T'}$  are comparable, the structure parameter is measured from a sonic anemometer/thermometer as well, rather than from the scintillometer. Data of three other heights are investigated as well: 3 m, 100 m and 180 m, to complete this study.

Firstly, we conclude that the turbulent temperature flux does not decrease linearly with height. For the 3 m flux lower values than for the 60 m and 100 m is observed in the afternoon. After correcting the 60 m, 100 m and 180 m level for the flux divergence, it seems that the 3 m turbulent temperature flux deviates from those fluxes. A possible reason for the deviation of the 3 m flux is that another footprint is measured, in which the soil is more moist. However, this is only one possible explanation. To confirm it our first recommendation is that more research is necessary to understand the different pattern of the 3 m turbulent temperature flux in the afternoon.

Secondly, we found that, as expected, MOST can be used to determine the surface turbulent temperature flux from the 3 m structure parameter of temperature. The structure parameter of temperature calculated from the turbulent temperature flux with MOST correlates well with the one measured with the sonic anemometer/ thermometer. Only a slight underestimation is found.

Thirdly, the structure parameter measured from the scintillometer has values comparable to those of the sonic anemometer/ thermometer at 60 m. Due to the path averaging of the scintillometer, the data give a smoother signal than the observations of the sonic anemometer/ thermometer.

Fourthly, when using the measured 3 m flux, the results do not agree with one of the two concepts. Investigating all the data in total, without distinguishing between morning and afternoon observations, higher correlation can be found if the structure parameter is calculated using MOST with the local (60 m, 100 m and 180 m) turbulent flux than the 3 m flux. In general, both methods of calculation underestimate the observed structure parameter of temperature. The morning transition between the stable and unstable conditions is measured at the some moment for the measured structure parameter and the structure parameter of temperature calculated with local turbulent flux. However, in the rest of the morning the use of 3 m gives the best results. In the afternoon, when the respective level is located in the surface layer, it does matter whether the 3 m or the local turbulent temperature flux is taken. This is related to the first conclusion.

Fifthly, we can conclude that an increase of height causes (a) less correlation between the observed structure parameter and the structure parameter calculated with the two MOST concepts, (b) an increase in the underestimation of the structure parameter calculated with MOST and (c) more variation between the observed similarity relation and the published equations. However, under very unstable conditions the data shows still a relation with the proposed formulas. These conclusions indicate that maybe not only surface processes are of interest, and MOST can be questioned here. Therefore, we recommend investigating whether other dimensionless scaling can improve the result, like for instance the local free convection scaling as is described by Wyngaard (1973).

Sixthly, using the surface flux from the 60 m flux, taking into account flux divergence between the surface and 60 m, gives more interpretable results. However, still neither of the two concepts gives the final answer. The morning transition observed as the minimum in the structure parameter calculated from the

MOST using the 60 m flux is at the same moment as the direct measured structure parameter of temperature. In the morning period the observed structure parameter of temperature lies between the structure parameter calculated with the two concepts. In the afternoon, the structure parameter of the two concepts is comparable with the observed one. Because of the better understandable results using the flux divergence corrected 60 m flux; we recommend to investigate this for the other levels as well. Furthermore, we would recommend analyzing (a) more days, or (b) with other statistical tools or (c) with Large Eddy Simulation, to further investigate whether of the two concepts give the right answer and to a better understanding of the behaviour of the structure parameter of temperature at higher levels.

## 6. Literature

- Andreas, E.L. (1988): *Estimating  $C_n^2$  over snow and seas ice from meteorological data*. Journal of the Optical Society of America **5**: 481-495
- Beljaars, A.C.M. (1982): *The derivation of fluxes from profiles in perturbed areas*, Boundary Layer Meteorology **24**: 35-55
- Beyrich, F. and Görsdorf, U. (1995), *Composing the diurnal Cycle of Mixing height from simultaneous sodar and windprofiler measurements*, Boundary-Layer Meteorology **76**: 387-394,
- Bosveld, F.C. (1999): *The KNMI Garderen Experiment: micro-meteorological observations 1988-1989. corrections*, KNMI Scientific report WR 99-03, De Bilt, the Netherlands, 52 pp
- De Bruin, H.A.R. (2005): *Atmosphere-Land Interactions*, Lecture notes Wageningen University, Wageningen, the Netherlands, 119 pp
- De Bruin, H.A.R., Kohsiek, W. and van den Hurk, B.J.J.M. (1993): *A verification of some methods to determine the fluxes of momentum, sensible heat, and water vapour using standard deviation and structure parameter of scalar meteorological quantities*. Boundary layer Meteorology **63**: 231-257
- Gill Instruments Ltd. (2002): *Omnidirectional (R3) & Asymmetric (R3A) Research Ultrasonic Anemometer*, User Manual, 1210-PS-0002, Hampshire, United Kingdom, 77 pp.
- Hartogensis, O.K., De Bruin, H.A.R. and Van de Wiel, B.J.H. (2002): *Displaced-beam small aperture scintillometer test. Part II: CASES-99 stable boundary-layer experiment*, Boundary Layer Meteorology **105**: 149-176
- Hill, R.J., Ochs, G.R., and Wilson, J.J. (1992): *Measuring surface-layer fluxes of heat and momentum using optical scintillation*. Boundary layer Meteorology **58**: 391-408
- Klein Baltink, H. and Holtslag, A.A.M. (1997): *A Comparison of Boundary-Layer Heights inferred from Wind profiler Backscatter Profiles with Diagnostic Calculations using Regional Model Forecasts*, Proceedings EURASAP Workshop, 1-3 October, 1997, Risø, Denemarken, 51-54.
- Kohsiek, W., Meijninger, W.M.L., de Bruin, H.A.R. and Beyrich, F. (2006): *Saturation of the large aperture scintillometer*, Boundary layer Meteorology **121**: 111-126
- Kohsiek, W., Meijninger, W.M.L., Moene, A.F., Heusinkveld, B.G., Hartogensis, O.K., Hillen, W.C.A.M. and de Bruin, H.A.R. (2002): *An extra large aperture scintillometer for long range applications*, Boundary Layer Meteorology **105**: 119-127
- Lee, X., Finigan, J and Kyaw, T.P.U. (2004): *Handbook of Micrometeorology, A Guide for Surface Flux Measurements and Analysis*, Kluwer Academic Publishers, The Netherlands, Dordrecht, 33-66
- Liu, H., Peters, G. and Foken, T. (2001): *New equations for sonic temperature variance and buoyancy heat flux with an omnidirectional sonic anemometer*, Boundary Layer Meteorology **100**: 459-468
- Meijninger, W.M.L. (2003): *Surface Fluxes over natural landscapes using scintillometry*, PhD thesis Wageningen University, Wageningen, the Netherlands
- Moene, A.F. and Van Dam, J.C. (2008): *Atmosphere-Vegetation-Soil Interactions*, Lecture notes Wageningen University, Wageningen, the Netherlands, 214 pp
- Moene, A.F., Meijninger, W.M.L., Hartogensis, O.K., Kohsiek, W. and De Bruin, H.A.R. (2004): *A review of the relation describing the signal of a Large Aperture Scintillometer*, Internal Report 2004/2, Meteorology and Air Quality Group, Wageningen University, Wageningen, the Netherlands, 40 pp.
- Nieuwstadt, F.T.M. (1984): *The turbulent structure of the stable, nocturnal boundary layer*, Journal of the Atmospheric Science **41**: 2202-2216
- Nieuwstadt, F.T.M. (1998): *Turbulentie, theorie en toepassingen van turbulente stromingen*, Epsilon Uitgaven, Utrecht, the Netherlands, 211 pp
- Schotanus, P., Nieuwstadt, F.T.M. and De Bruin, H.A.R. (1983): *Temperature measurement with a sonic anemometer and its application to heat and moisture fluxes*, Boundary Layer Meteorology **26**: 81-93
- Stull, R.B. (1988): *An Introduction to Boundary Layer Meteorology*, Kluwer Academic Publishers, The Netherlands, Dordrecht, 666pp
- Wyngaard, J. C. (1973): *On Surface-Layer turbulence*. In: Haugen D.A. Workshop on Micrometeorology, Boston, Mass. American Meteorological Society, pp 101-149
- Wyngaard, J.C., Izumi, Y. and Collins, S.A. (1971): *Behavior of the Refractive-Index-Structure Parameter near the Ground*, Journal of the Optical Society of America **61**: 1646-1650



